Supporting Information

Syntheses and studies of electron/energy transfer of new dyads based on an unsymmetrical perylene diimide incorporating chelating 1,10-phenantroline and its corresponding square-planar complexes with dichloroplatinum(II) and dichloropalladium(II)

Sebile Işık Büyükekşi[a], Ahmet Karatay[b], Nursel Acar[c], Betül Küçüköz[b], Ayhan Elmalı[b] and Abdurrahman Şengül[a*]

[a]*Department of Chemistry, Faculty of Arts and Sciences, Bülent Ecevit University, 67100 Zonguldak, Turkey*

[b]*Department of Engineering Physics, Faculty of Engineering, Ankara University, 06100 Beşevler, Ankara, Turkey*

[c]*Department of Chemistry, Faculty of Science, Ege University, 35100 Bornova, Izmir, Turkey*

[*]Corresponding author. Tel: +90 372 2911126; fax: +90 372 257 4181.

E-mail address: abdurrahmans2002@yahoo.co.uk sengul@beun.edu.tr (A. Sengul)

Table of Contents

Synthesis of PDI-3

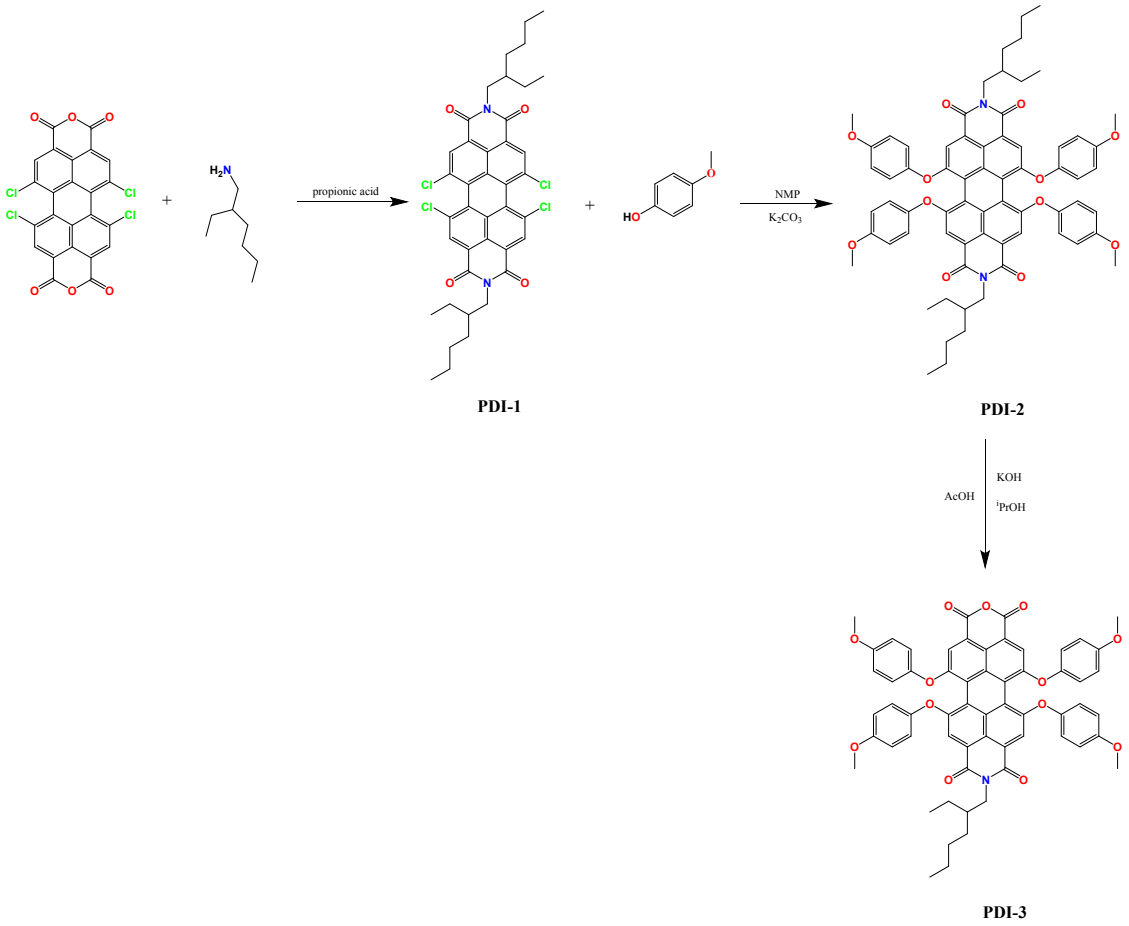

Scheme S1. Synthesis of **PDI-3**.

*N'-(2-ethylhexyl)-1,6,7,12-tetrakis-(4-methoxyphenoxy)perylene-9,10-dicarboxylicimide-3,4-dicarboxylic anhydride (**PDI-3**)*

N,*N*'-di(2-ethylhexyl)-1,6,7,12-tetrakis-(4-methoxyphenoxy)perylene-3,4,9,10-tetracarboxylic acid diimide (4.6 g, 1.49 mmol) and KOH (4.9 g) were heated under reflux for 70 min. in a mixture of isopropanol (48 mL) and H_2O (6 mL). After cooling the reaction mixture to room temperature, it was stirred in acetic acid (10 mL) for 1h, H_2O was added, and the resulting precipitate was filtered and dried under vacuum. The crude product was purified by column chromatography on silica gel using (DCM/EtAs – 100/1) as eluent. The product (0.29 g, 20%) was obtained as a purple solid. FT-IR Spectrum [(ATR)/cm^{-1}]: 3075 (Ar-CH), 2956-2850 (CH), 1765 (C=O anhydride), 1735 (C=O anhydride), 1662 (C=O imide), 1589 (C=C), 1499, 1463, 1442, 1407, 1394, 1376, 1339, 1285, 1246, 1224, 1197 (C-O-C), 1179 (C-O-C), 1138, 1118, 1102, 1072, 1132, 1007, 946, 905, 873, 828, 796, 758, 742, 730, 705, 669, 650. MALDI-TOF (*m/z*): Calculated: 992.03; Found: 992.4 [M]$^+$. ^{1}H NMR (600 MHz, $CDCl_3$) δ_{ppm}: δ = 8.11 (s, 2H, H_{P1}), 8.08 (s, 2H, $H_{P1'}$), 6.92 (d, 8H, H_{P2}), 6.83 (d, 8H, H_{P3}), 4.03 (m, 2H, H_{H1}), 3.81 (s, 12H, H_{P4}), 1.54 (t, 1H, H_{H2}), 1.31-1.25 (m, 8H, $H_{H3, H5, H6, H7}$), 0.92-0.86 (m, 6H, $H_{H4, H8}$). ^{13}C NMR (DEPT, 600 MHz, $CDCl_3$) δ_{ppm}: (C) 163.633, 157.273, 156.905, 156.844, 148.170, 123.066, 121.403, 119.043, 117.939 (CH) 121.533, 121.449, 120.529, 118.782, 115.311, 115.265, 38.061 (CH_2) 44.413, 30.796, 29.685, 24.053, 23.033 (CH_3) 55.693, 55.678, 16.888, 10.581.

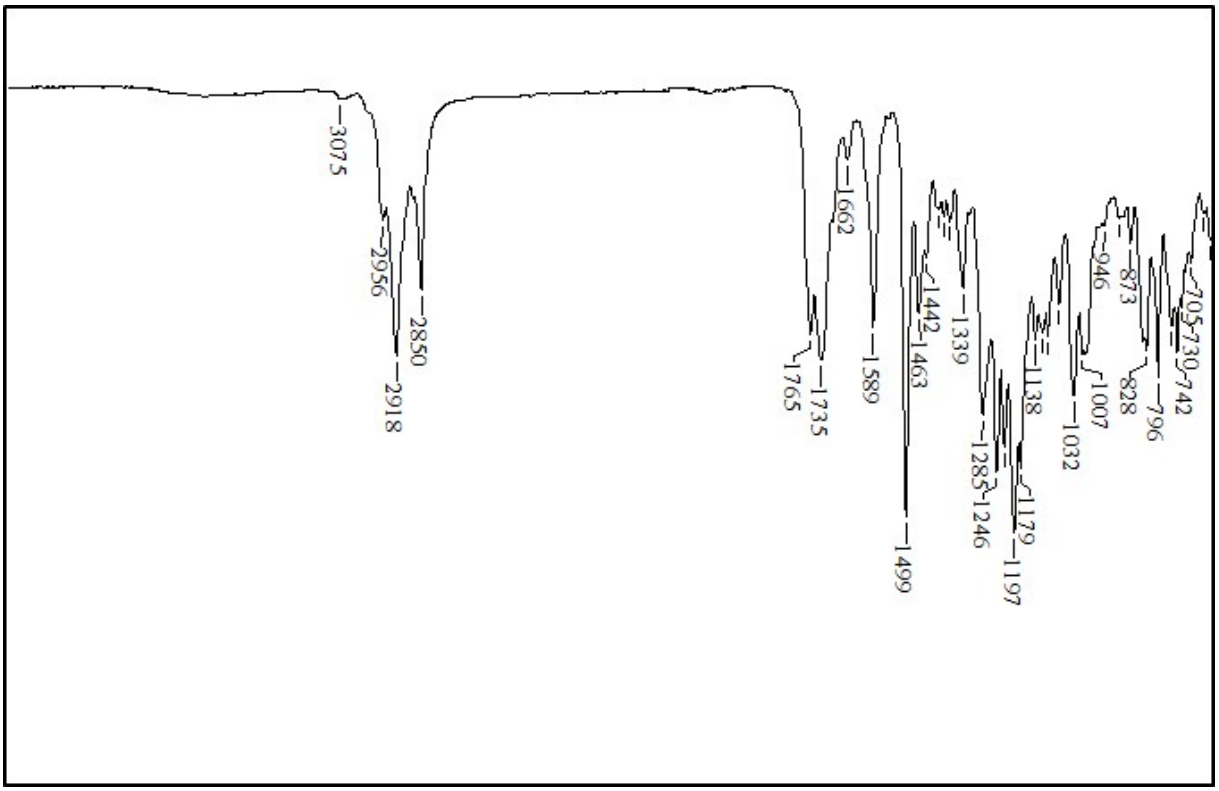

Figure S1. FT-IR spectrum of **PDI-3**

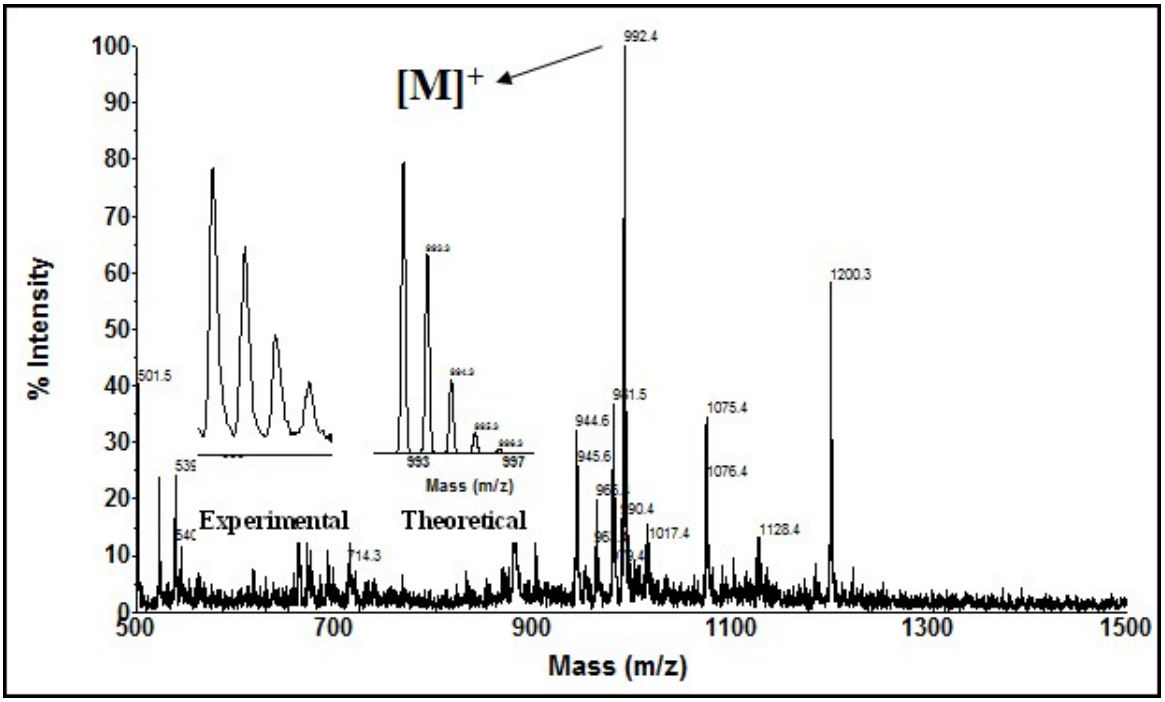

Figure S2. MALDI-TOF spectrum of **PDI-3**

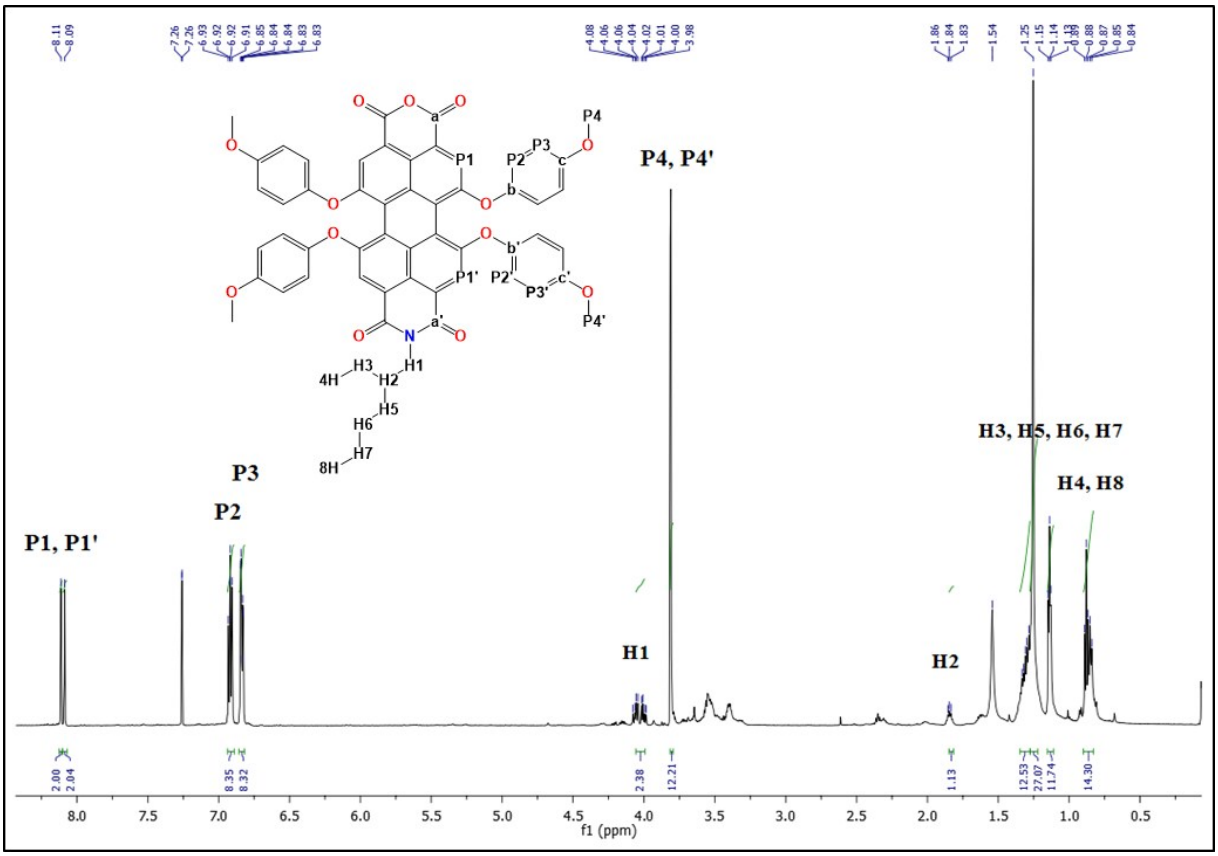

Figure S3. ^{1}H NMR spectrum of **PDI-3**

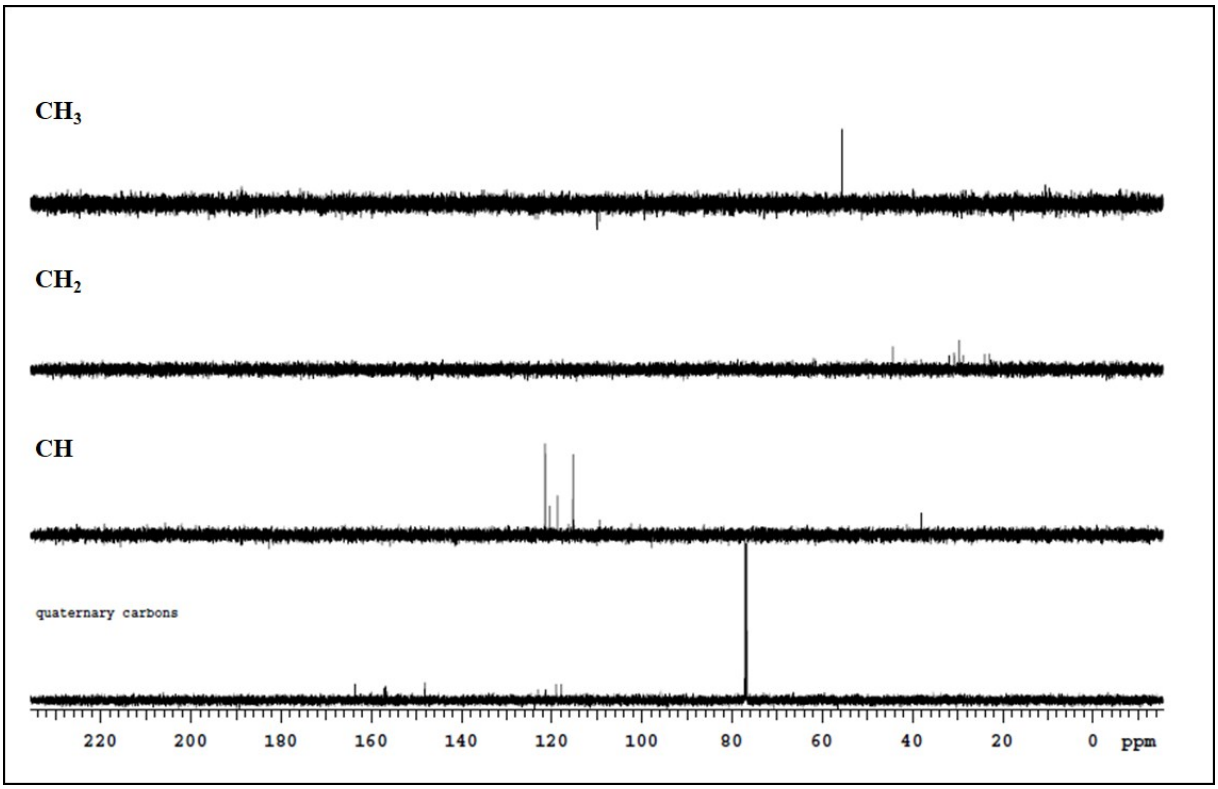

Figure S4. ^{13}C NMR DEPT spectrum of **PDI-3**

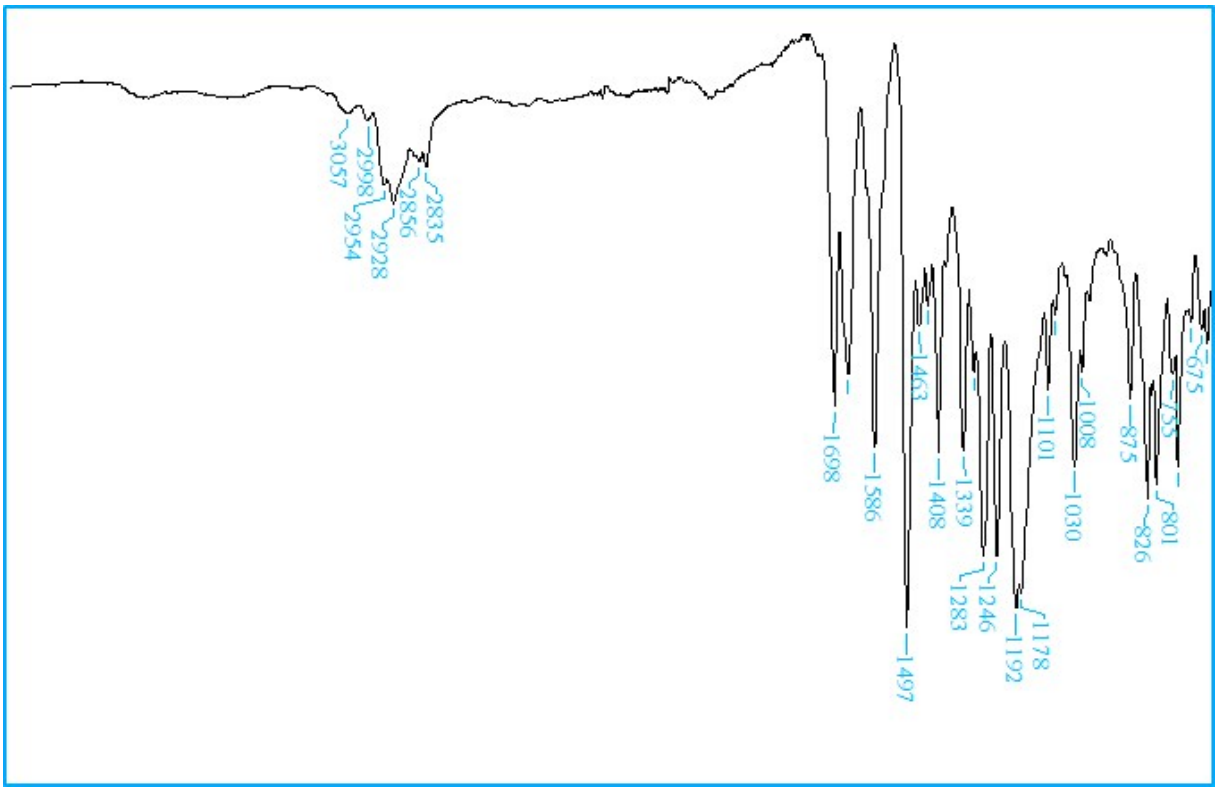

Figure S5. FT-IR spectrum of **1**

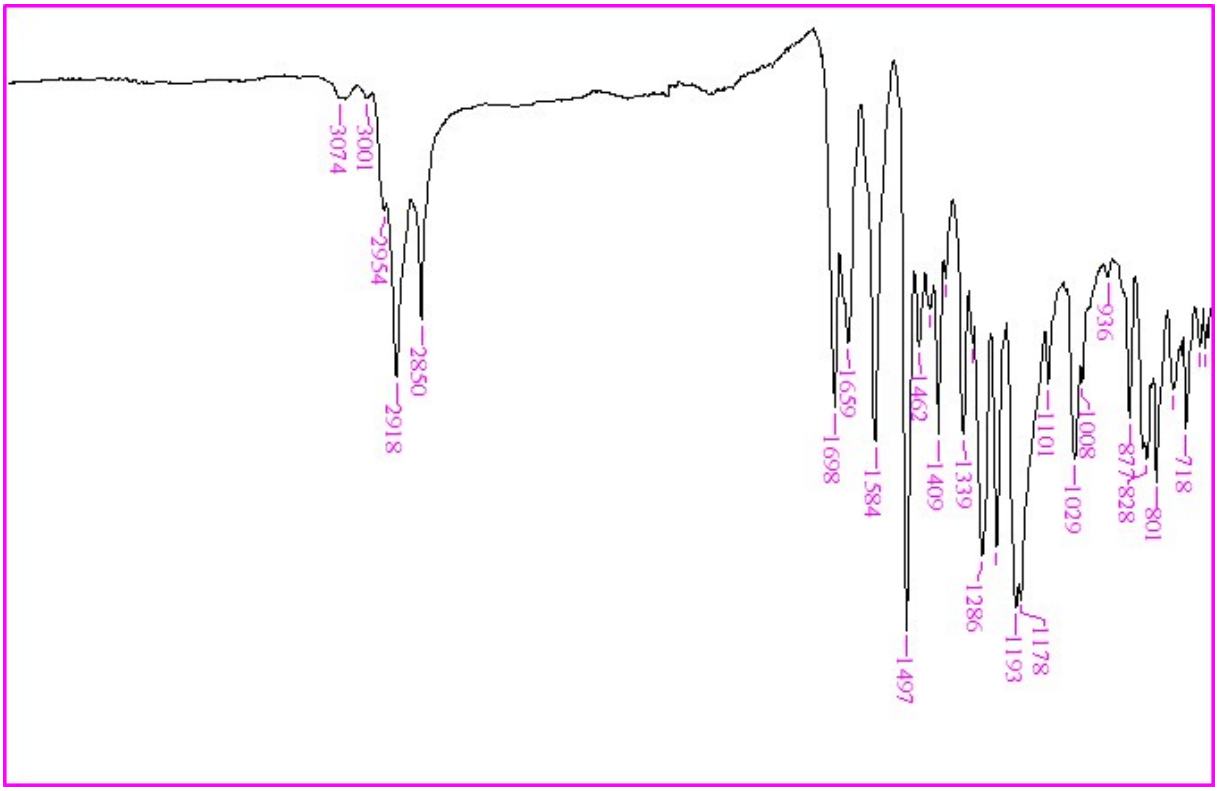

Figure S6. FT-IR spectrum of **2**

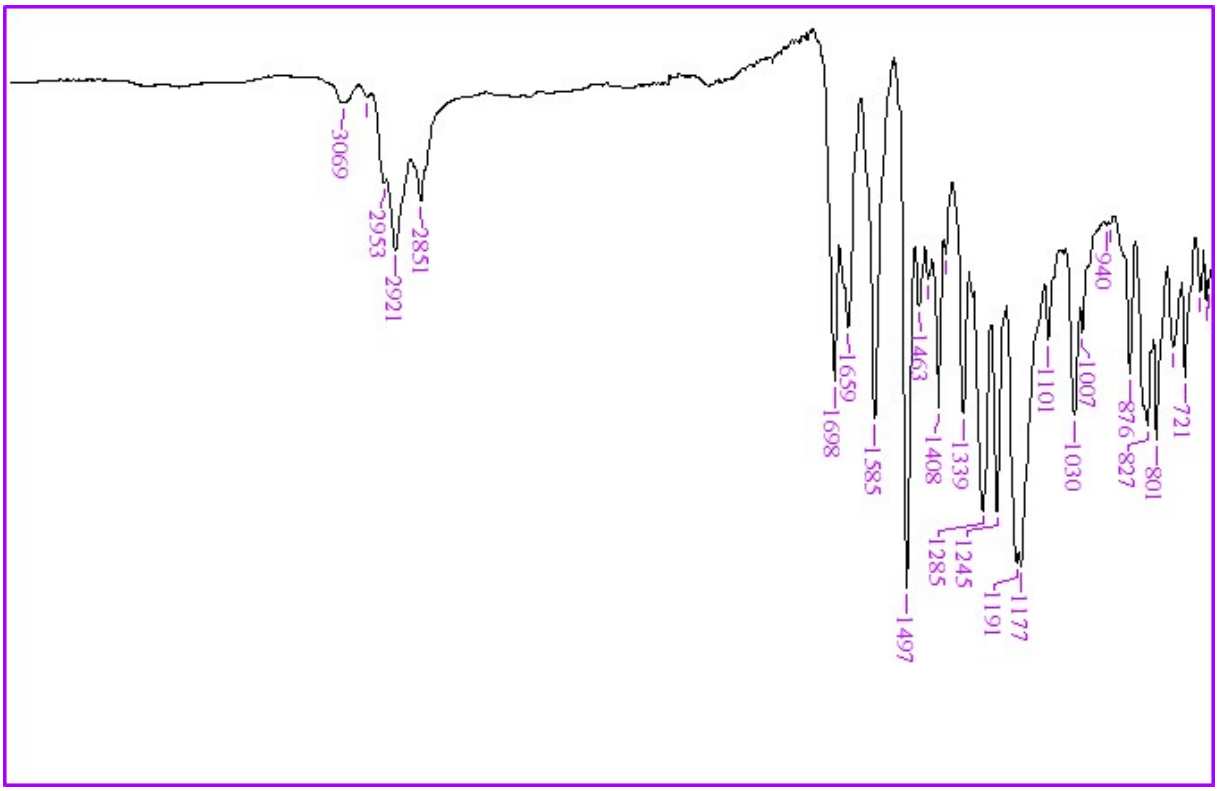

Figure S7. FT-IR spectrum of **3**

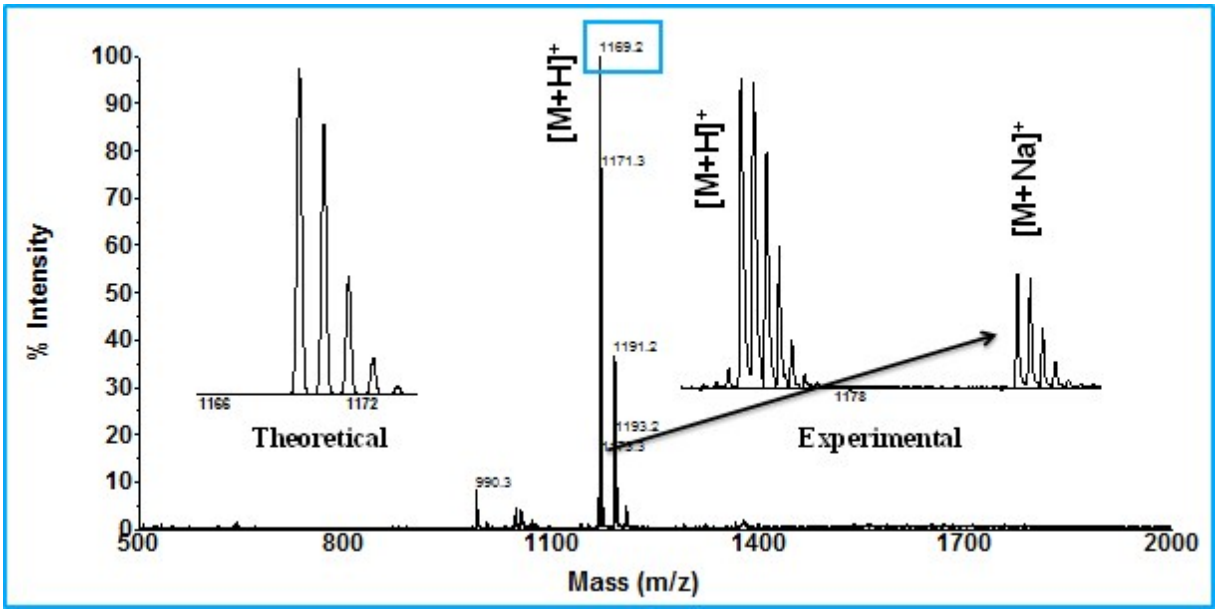

Figure S8. MALDI-TOF spectrum of **1**

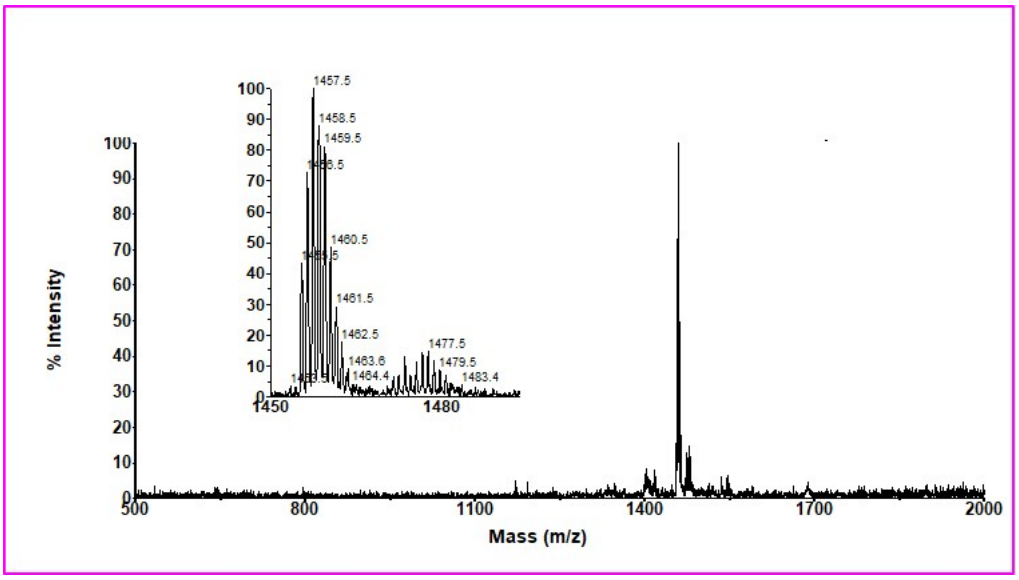

Figure S9. MALDI-TOF spectrum of **2**

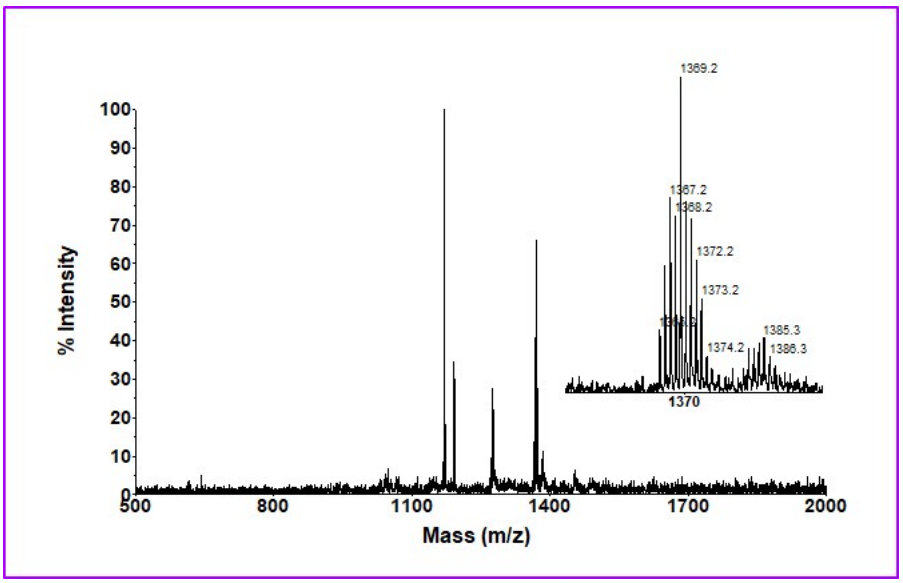

Figure S10. MALDI-TOF spectrum of **3**

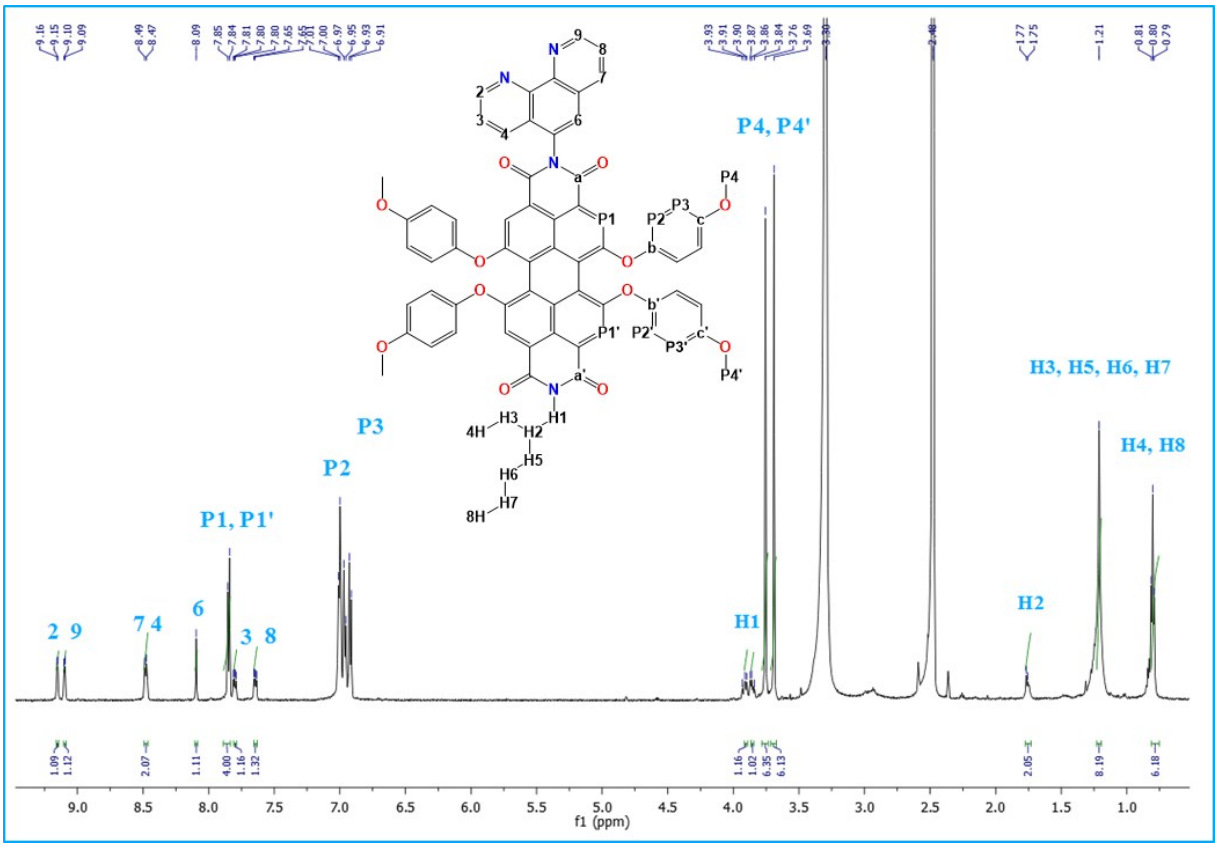

Figure S11. ^{1}H NMR spectrum of **1**

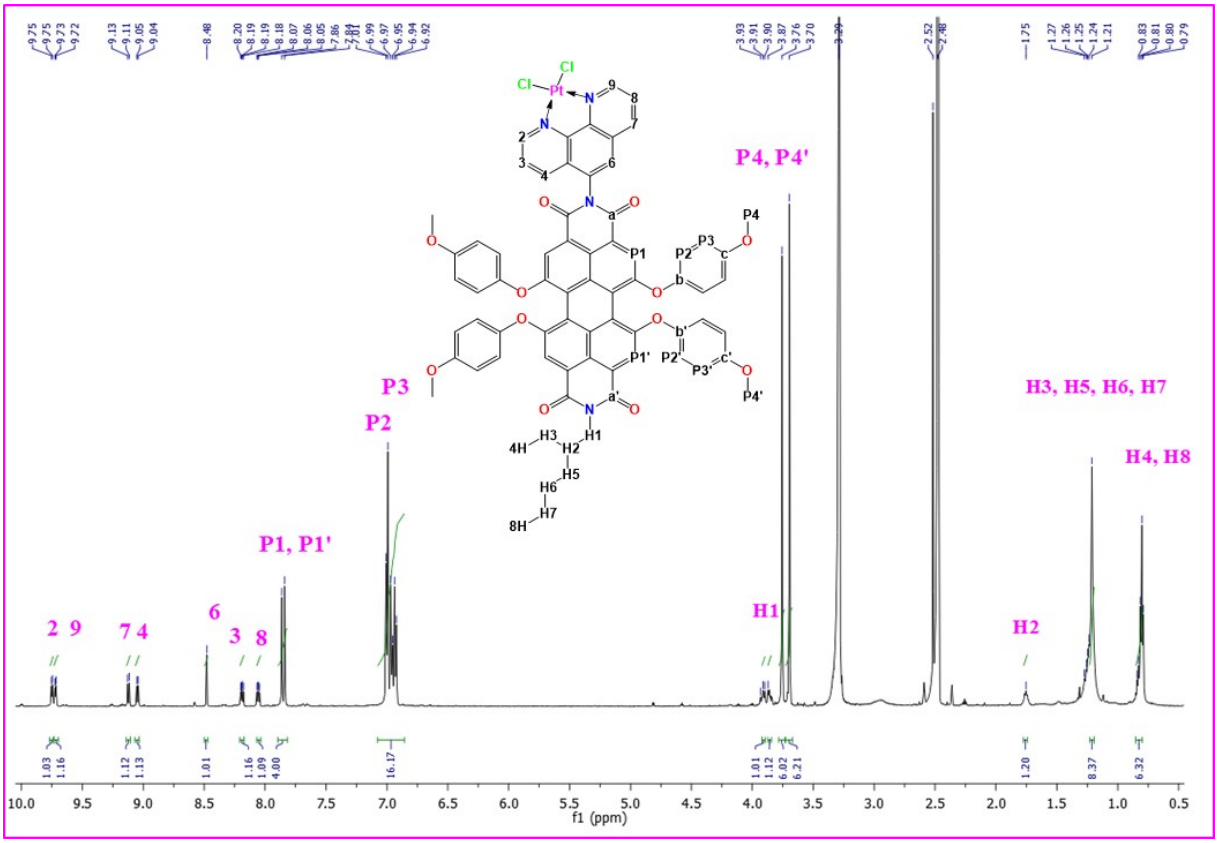

Figure S12. ^{1}H NMR spectrum of **2**

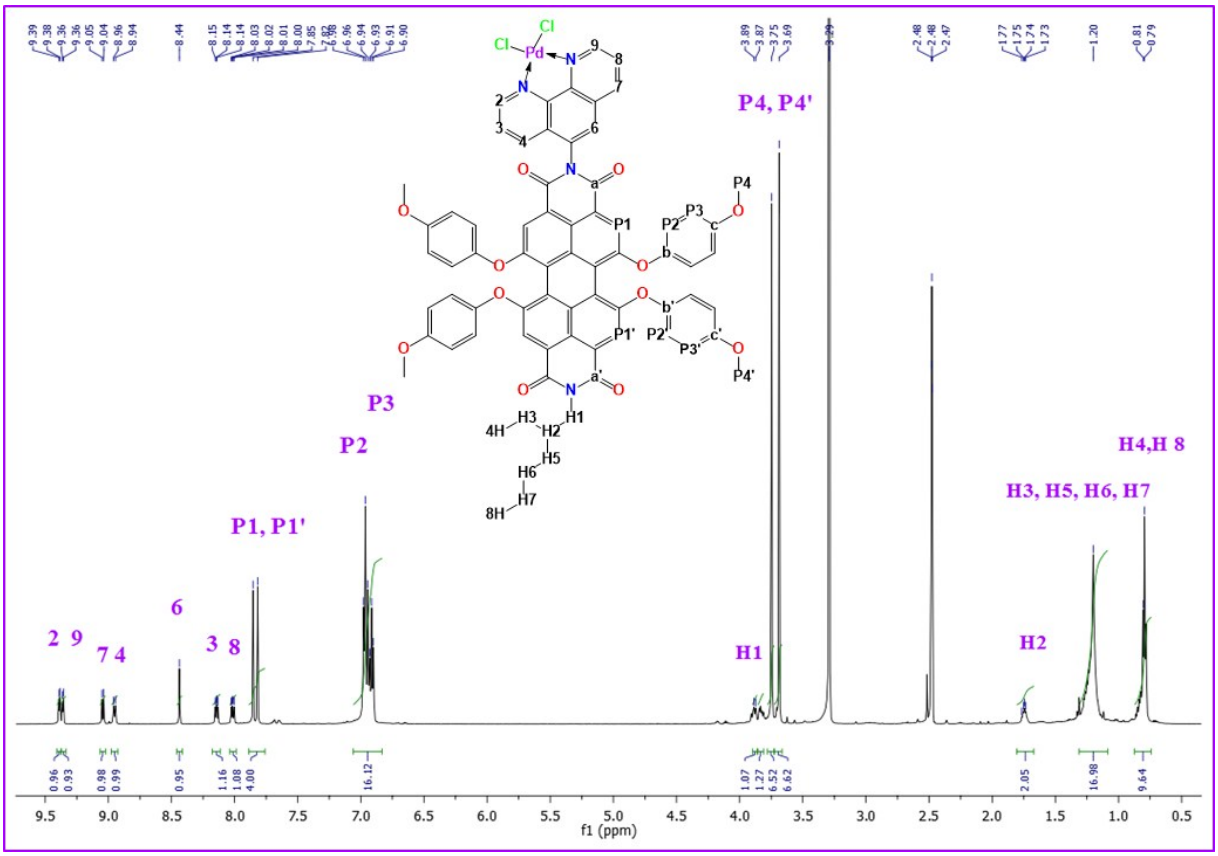

Figure S13. [1]H NMR spectrum of **3**

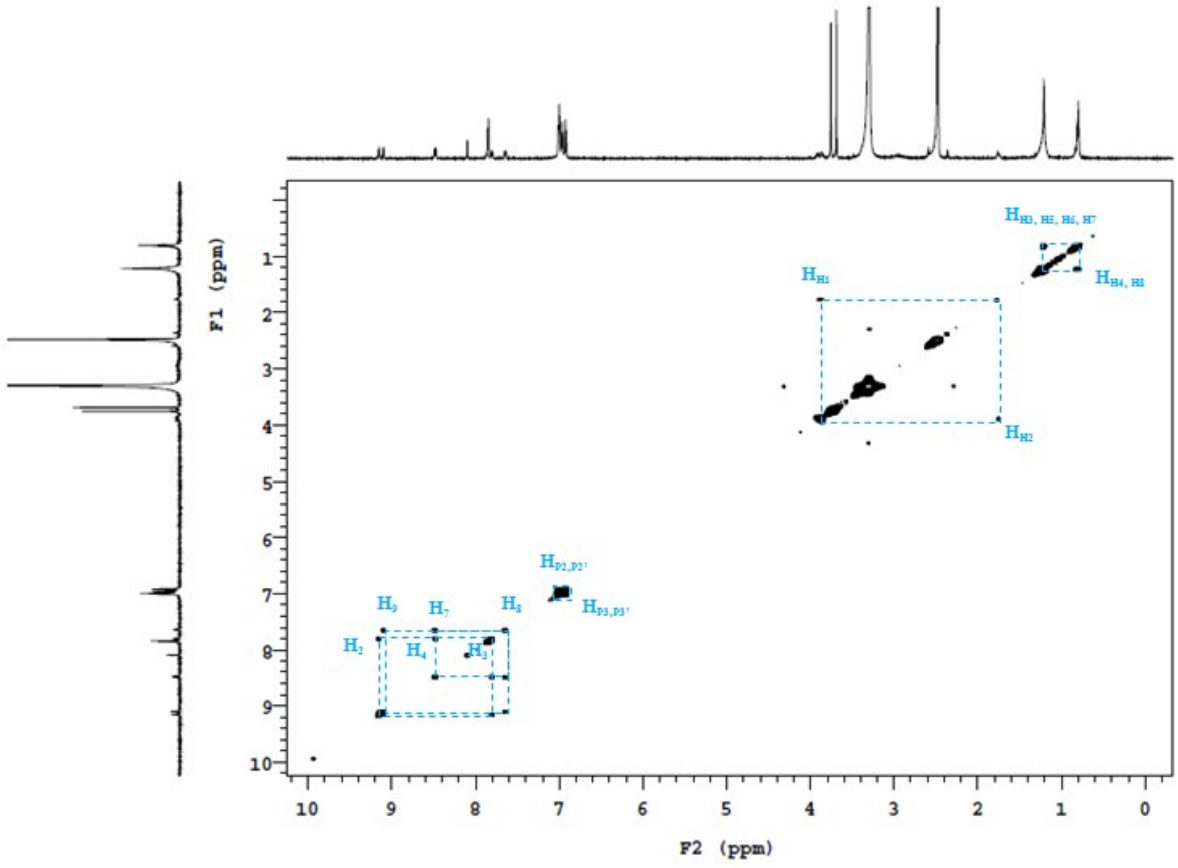

Figure S14. COSY spectrum of **1**

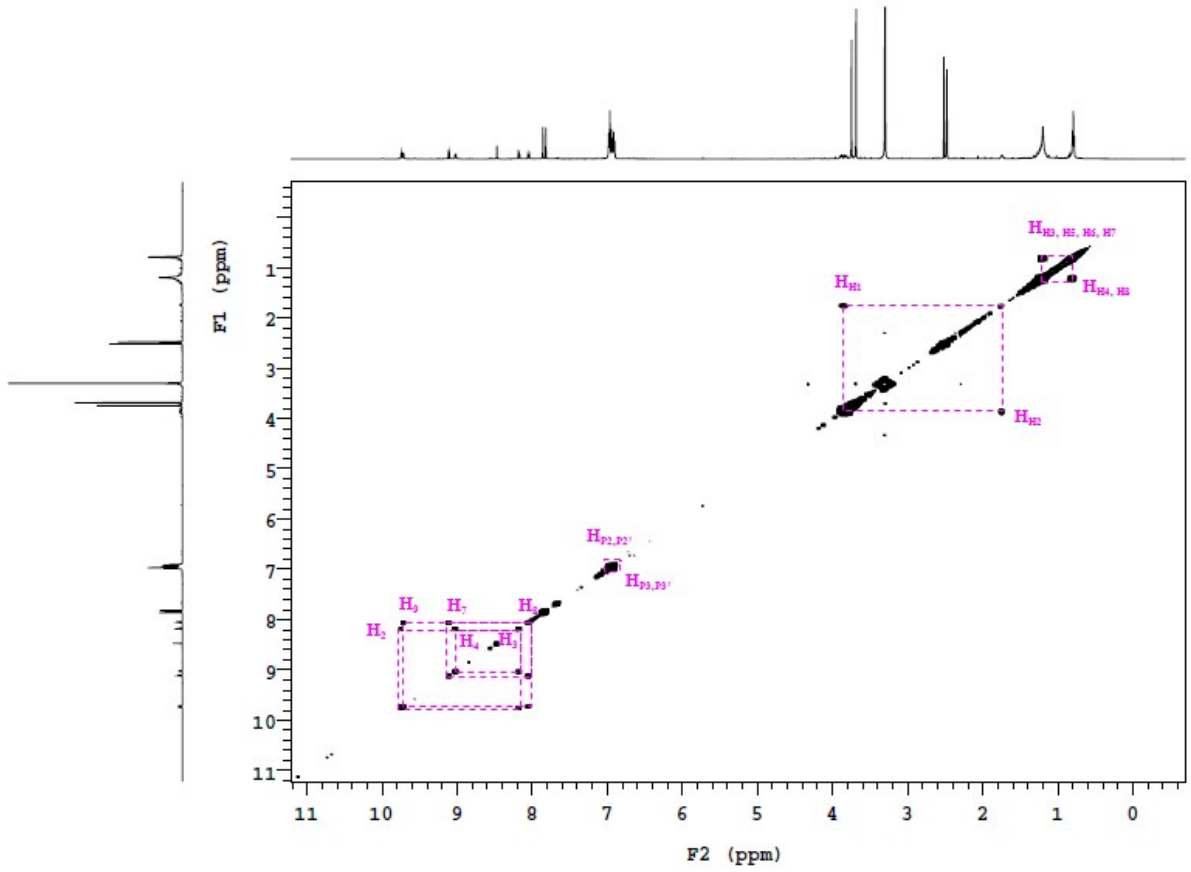

Figure S15. COSY spectrum of **2**

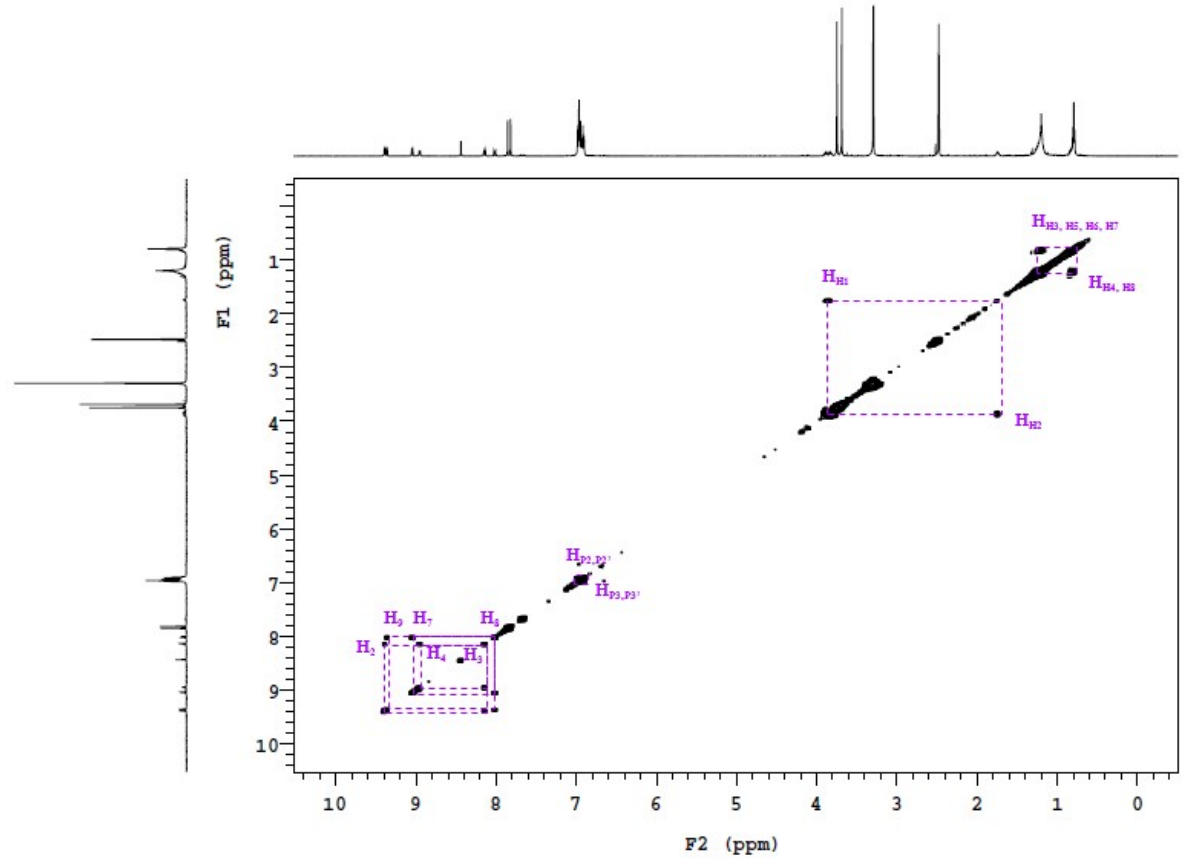

Figure S16. COSY spectrum of **3**

Table S1. ^{1}H chemical shifts (ppm) for compounds **1**, **2** and **3** in DMSO-d_6

	1	**2**	**3**
Proton	δ_H, *J* in Hz	δ_H, *J* in Hz	δ_H, *J* in Hz
H_{P1}	7.85 (s, 2H)	7.86 (s, 2H)	7.85 (s, 2H)
$H_{P1'}$	7.84 (s, 2H)	7.84 (s, 2H)	7.82 (s, 2H)
H_{P2} $H_{P2'}$	7.00 (m, 8H)	7.01 (m, 8H)	6.98 (m, 8H)
H_{P3} $H_{P3'}$	6.95 (m, 8H)	6.95 (m, 8H)	6.93 (m, 8H)
H_{P4}	3.76 (s, 6H)	3.76 (s, 6H)	3.75 (s, 6H)
$H_{P4'}$	3.69 (s, 6H)	3.70 (s, 6H)	3.69 (s, 6H)
H_2	9.16 (d, *J* = 3.89, 1H)	9.75 (d, *J* = 5.53, 1H)	9.39 (d, *J* = 5.27, 1H)
H_3	7.80 (dd, *J* = 4.08, 1H)	8.19 (dd, *J* = 5.59, 1H)	8.14 (dd, *J* = 5.52, 1H)
H_4	8.47 (m, 1H)	9.05 (d, *J* = 8.17, 1H)	8.96 (d, *J* = 8.15, 1H)
H_6	8.09 (s, 1H)	8.48 (s, 1H)	8.44 (s, 1H)
H_7	8.49 (m, 8H)	9.13 (d, *J* = 8.53, 1H)	9.05 (d, *J* = 8.47, 1H)
H_8	7.64 (dd, *J* = 4.11, 1H)	8.07 (dd, *J* = 5.55, 1H)	8.02 (dd, *J* = 5.39, 1H)
H_9	9.10 (d, *J* = 4.07, 1H)	9.73 (d, *J* = 5.52, 1H)	9.36 (d, *J* = 5.13, 1H)
H_{H1}	3.87 (m, 2H)	3.89 (m, 2H)	3.84 (m, 2H)
H_{H2}	1.75 (m, 1H)	1.75 (m, 1H)	1.74 (m, 1H)
$H_{H3,H5,H6,H7}$	1.21 (m, 8H)	1.21 (m, 8H)	1.20 (m, 8H)
$H_{H4,H8}$	0.80 (m, 6H)	0.80 (m, 6H)	0.79 (m, 6H)

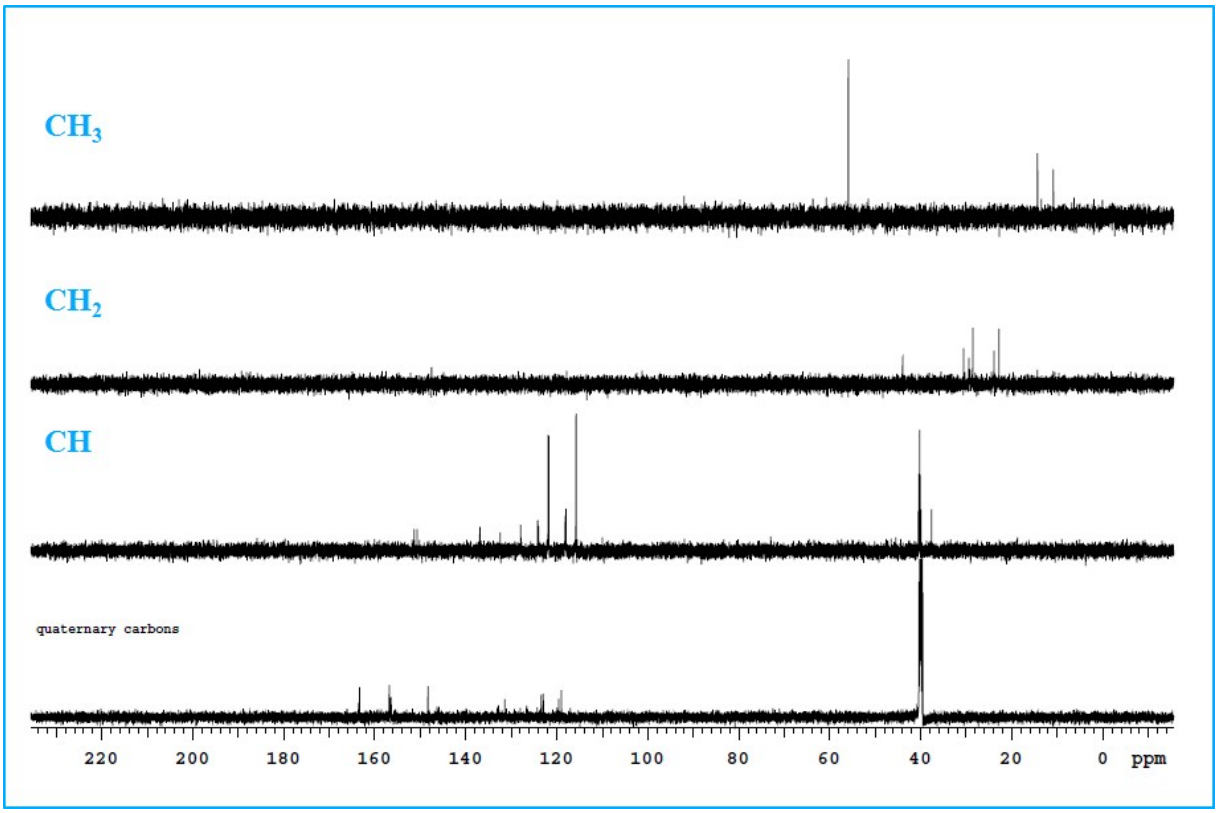

Figure S17. ^{13}C NMR DEPT spectrum of **1**

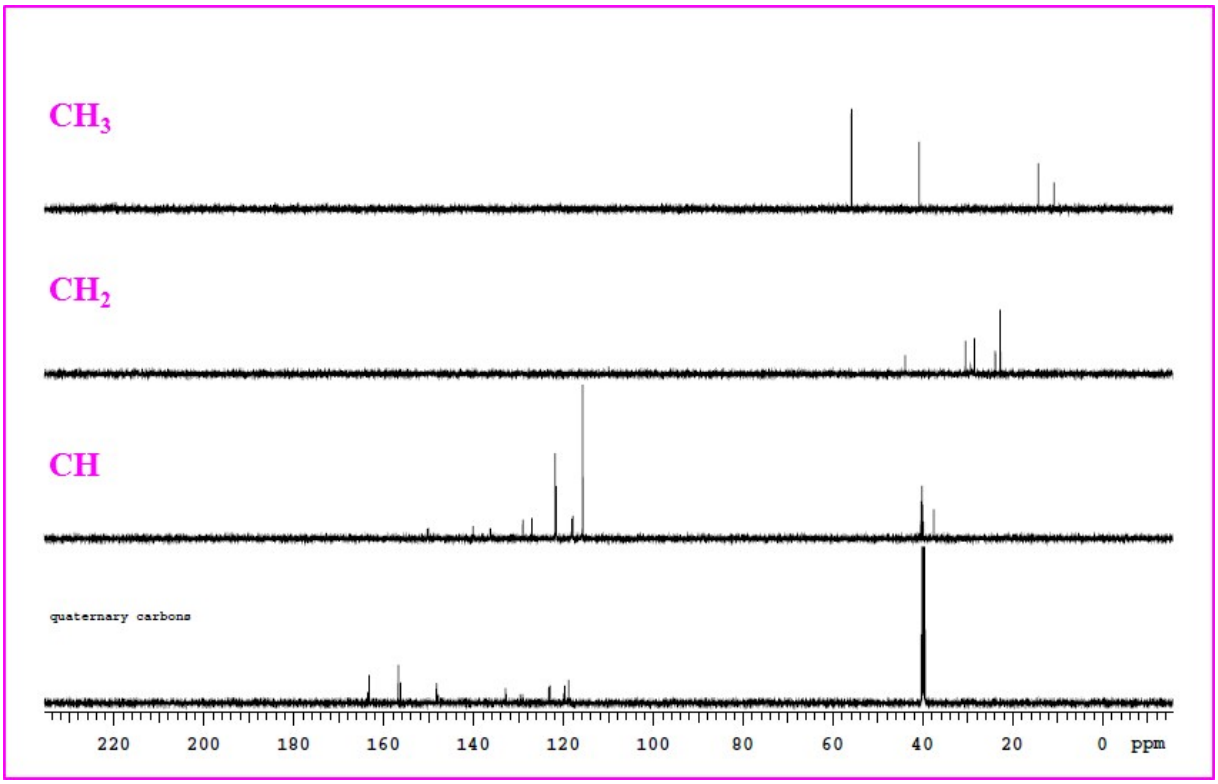

Figure S18. ^{13}C NMR DEPT spectrum of **2**

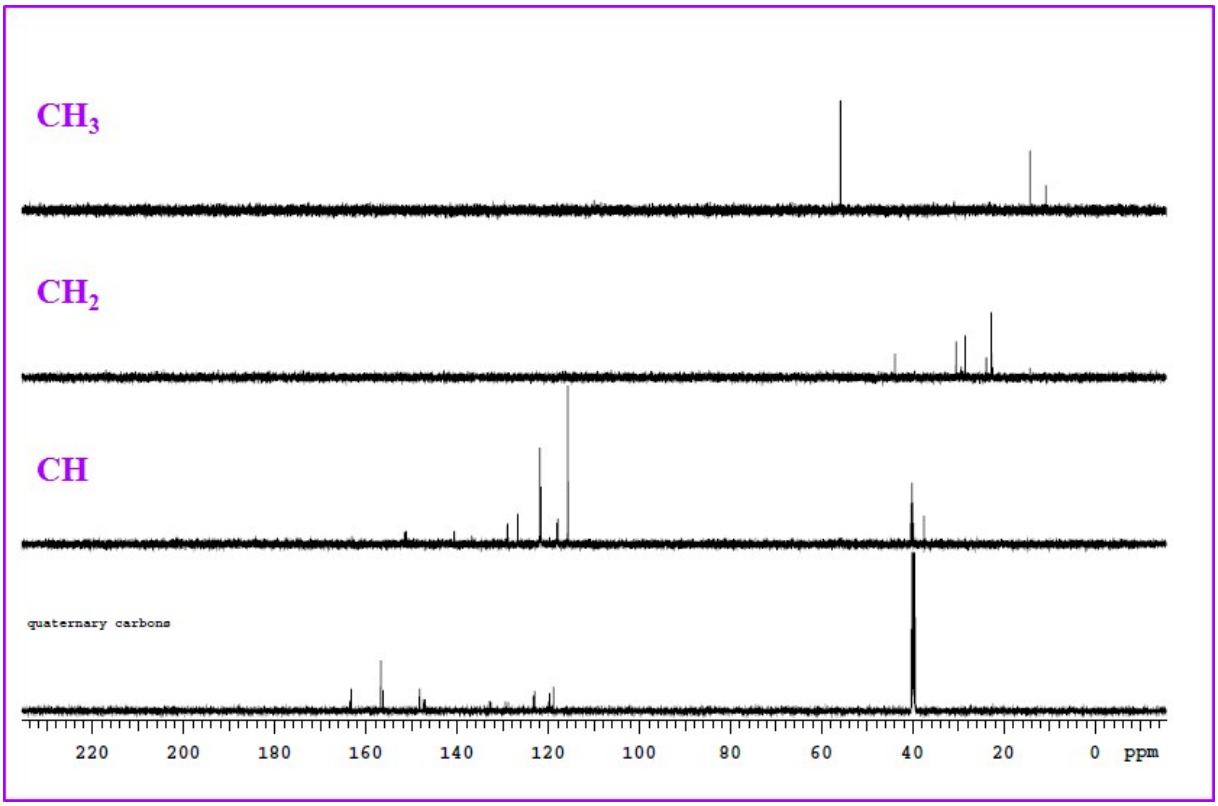

Figure S19. ^{13}C NMR DEPT spectrum of **3**

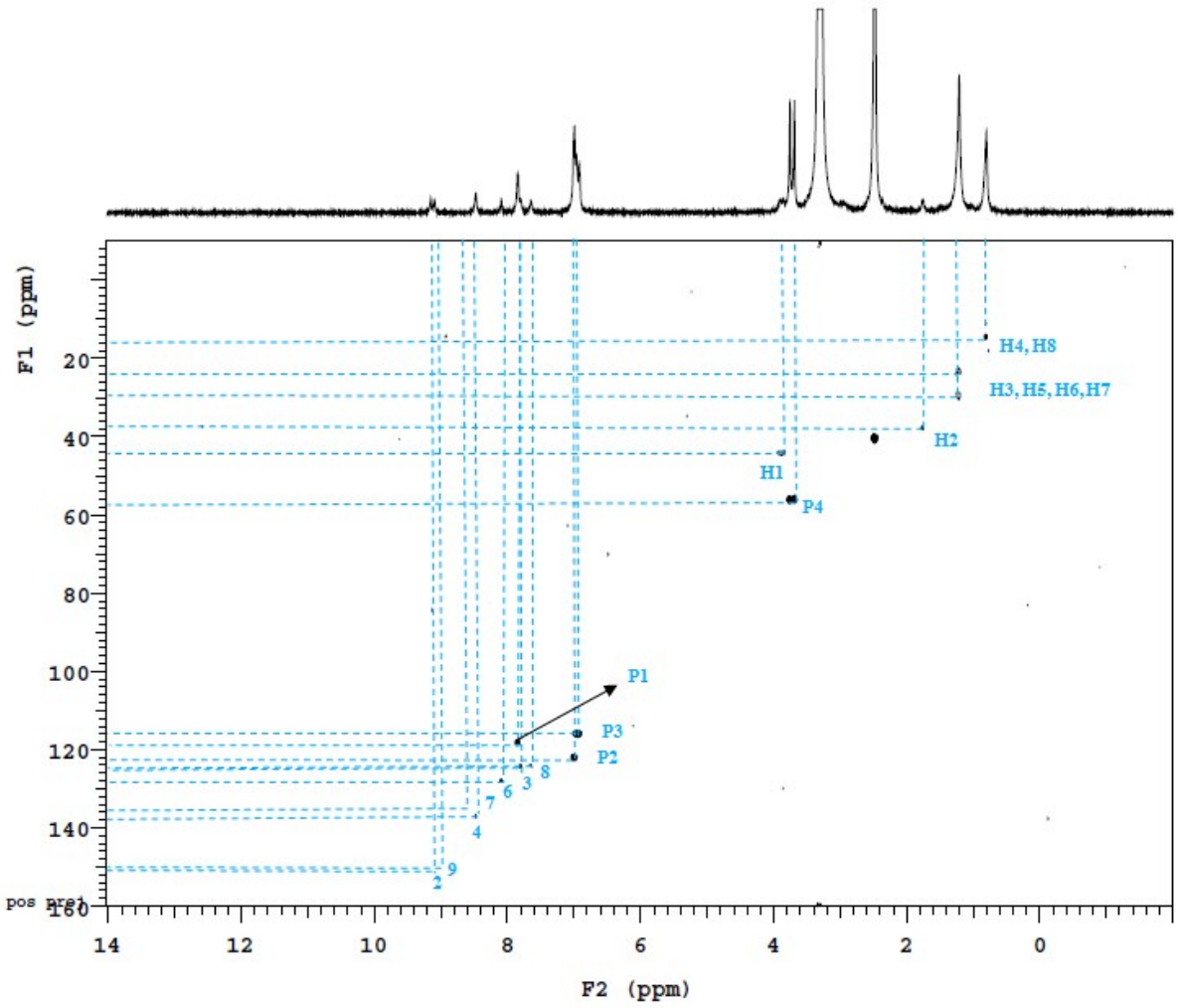

Figure S20. HSQC spectrum of **1**

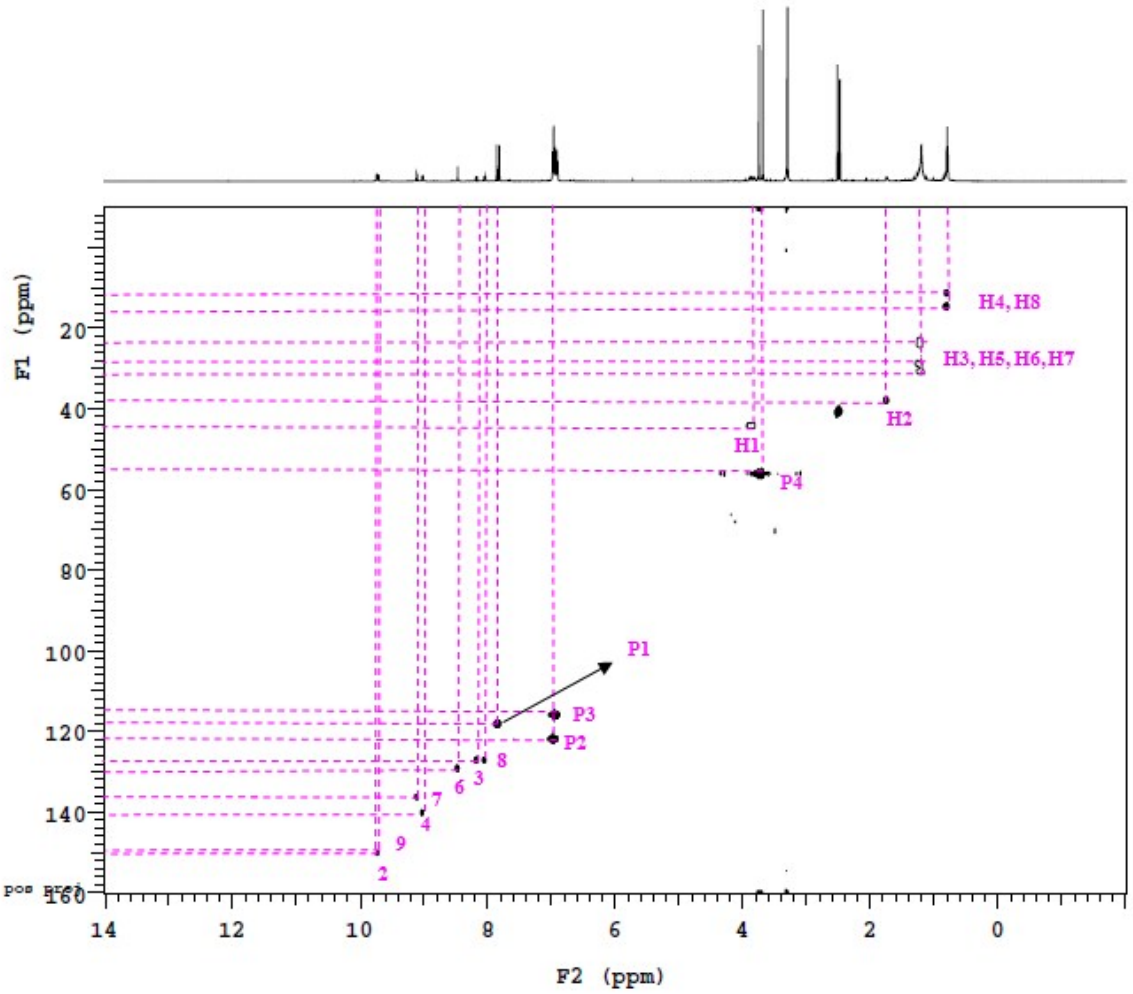

Figure S21. HSQC spectrum of **2**

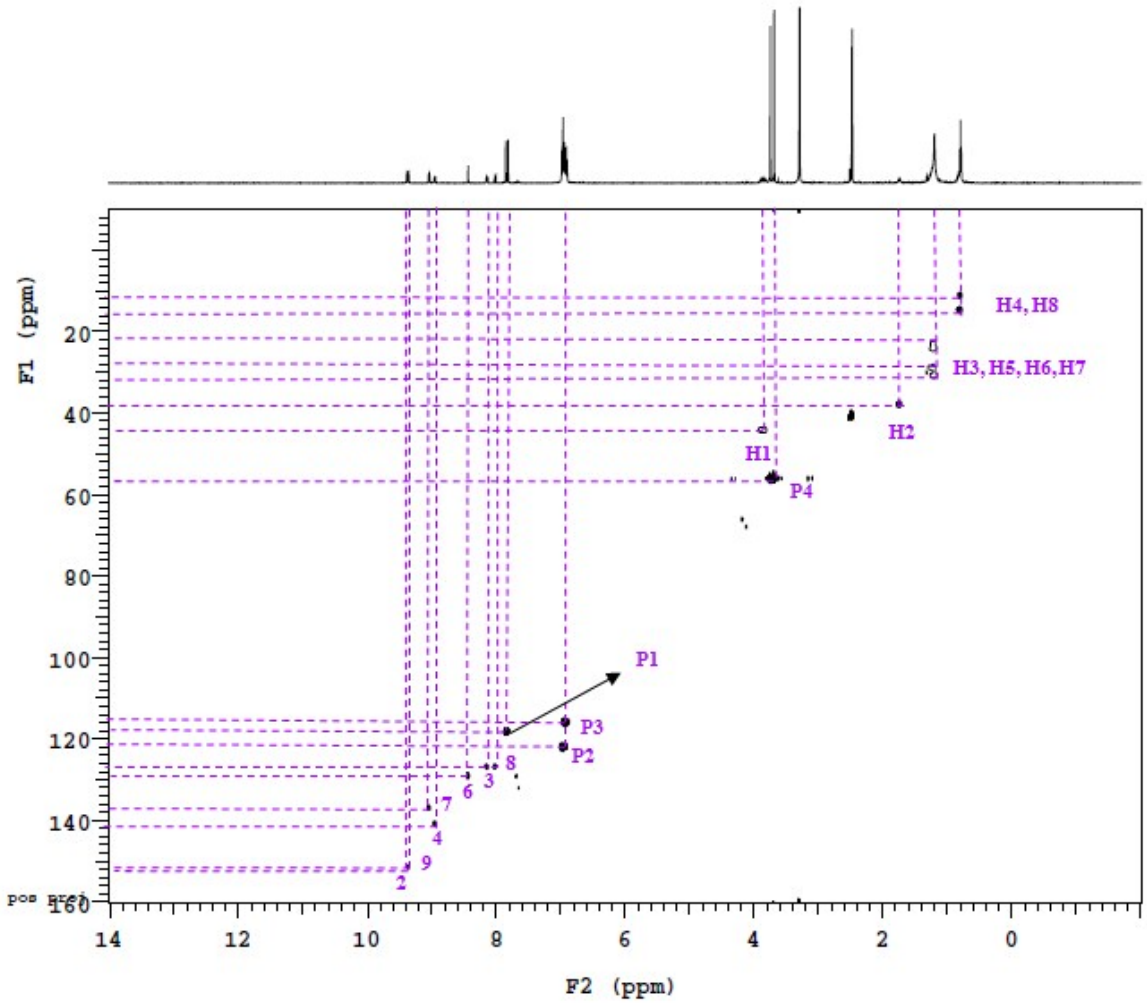

Figure S22. HSQC spectrum of **3**

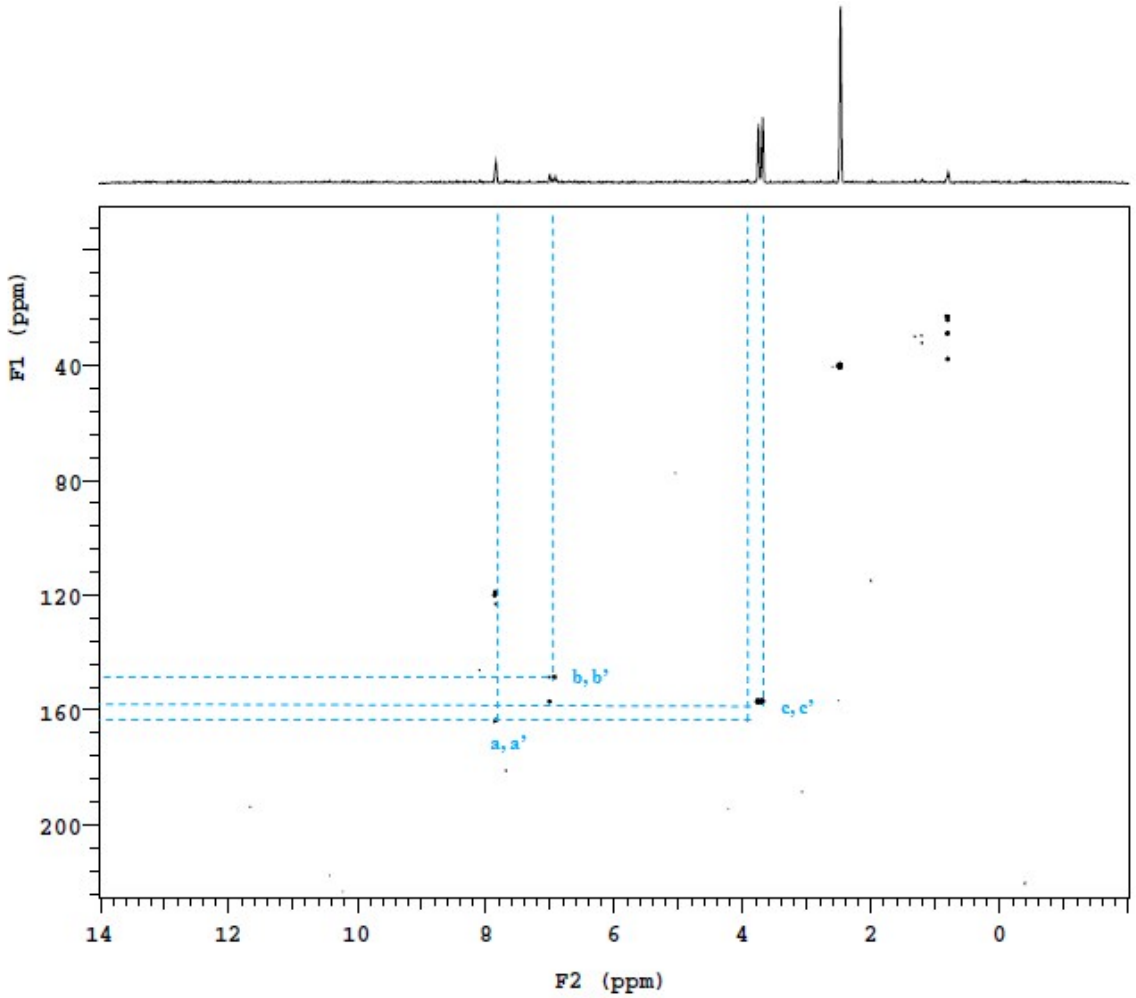

Figure S23. HMBC spectrum of **1**

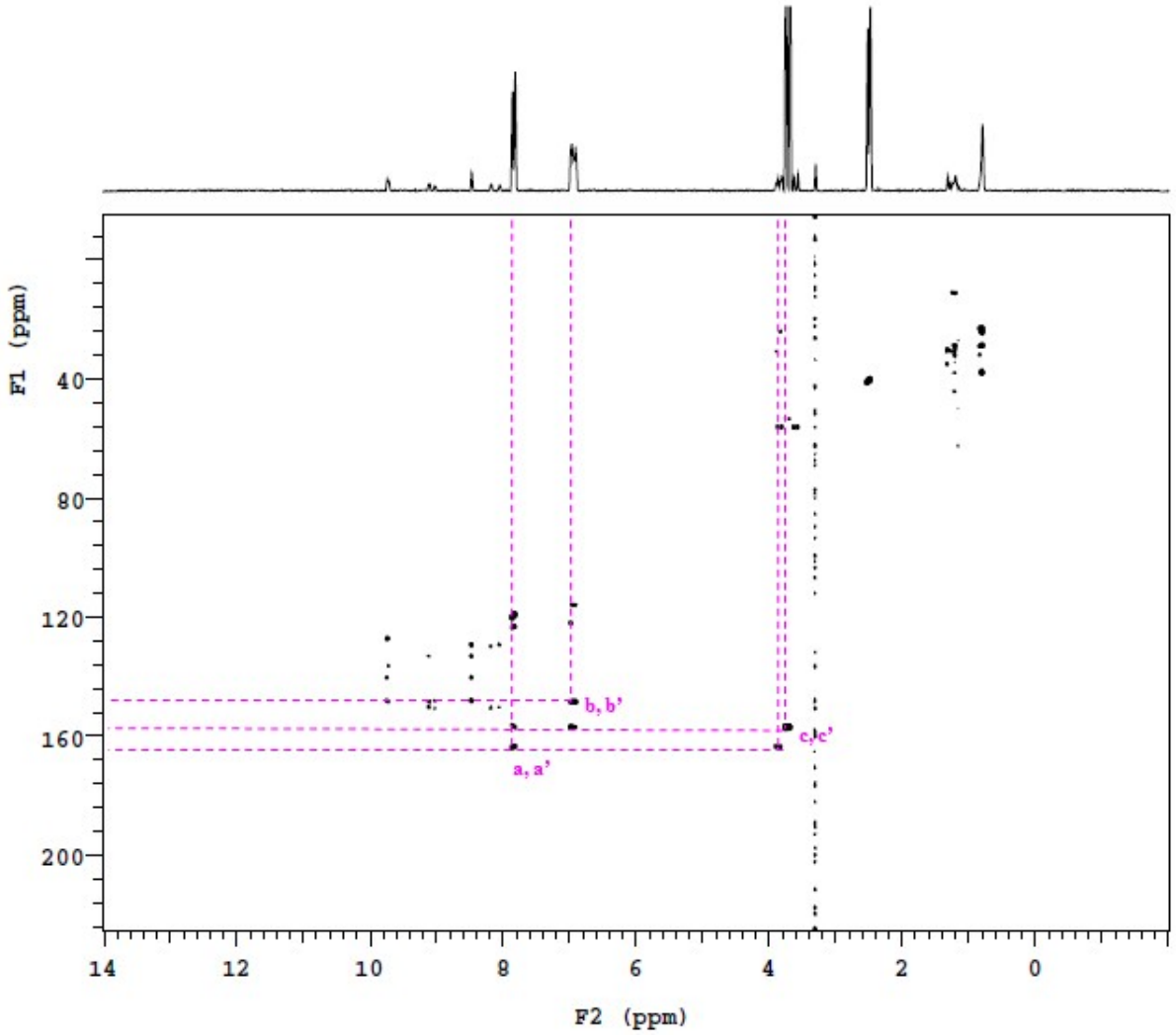

Figure S24. HMBC spectrum of **2**

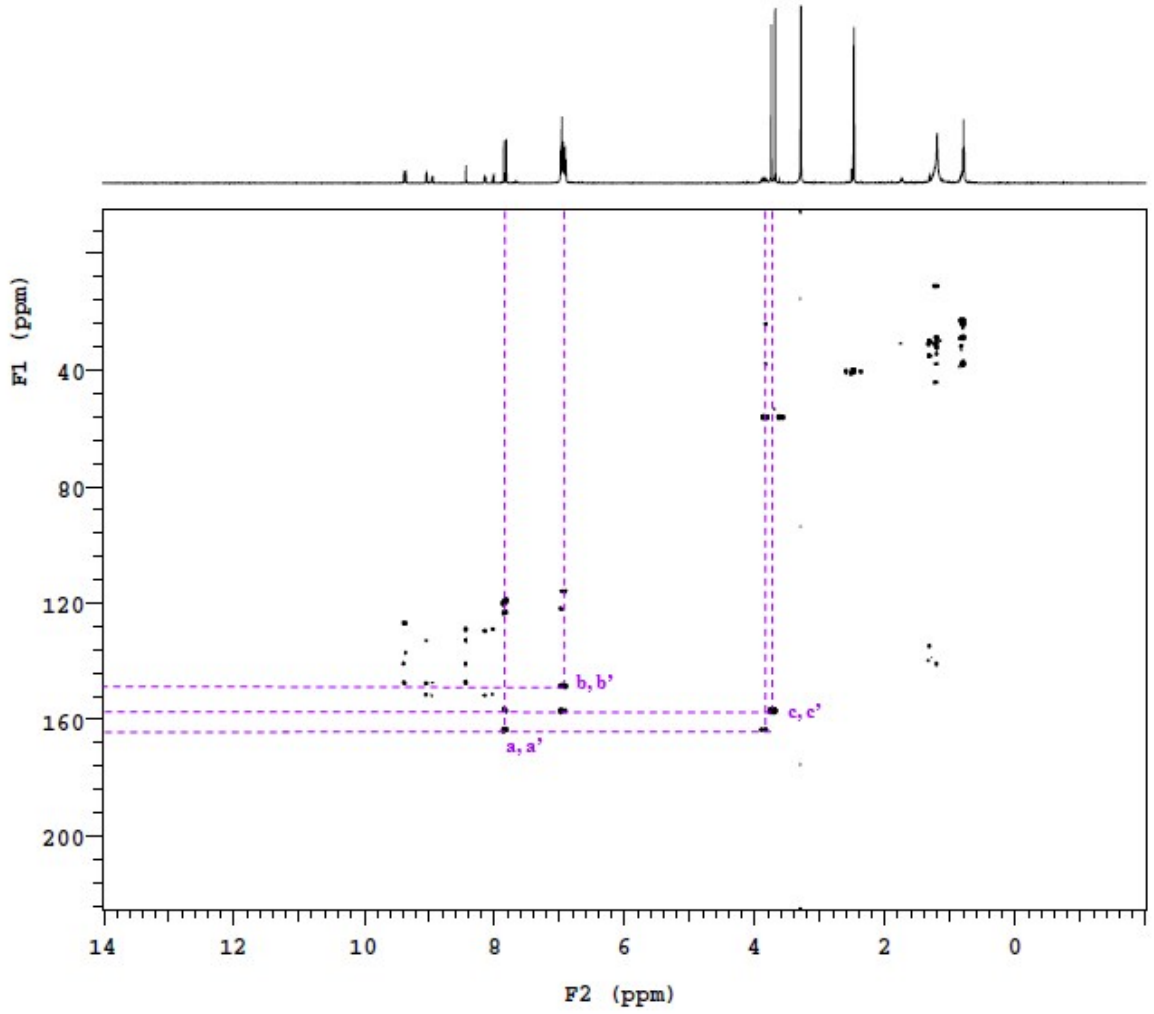

Figure S25. HMBC spectrum of **3**

Table S2. ^{13}C chemical shifts (ppm) for compounds **1**, **2** and **3** in DMSO-d_6

	1	**2**	**3**
Carbon	□C	□C	□C
C_{P1}	118.153	118.176	118.169
$C_{P1'}$	117.992	117.969	117.969
C_{P2}	121.908	121.901	121.901
$C_{P2'}$	121.770	121.694	121.694
C_{P3}	115.793	115.770	115.770
$C_{P3'}$	115.755	115.770	115.770
C_{P4}	55.945	55.953	55.953
$C_{P4'}$	55.907	55.922	55.914
C_a	163.564	163.580	163.564
$C_{a'}$	163.342	163.304	163.304
C_b	148.369	148.346	148.346
$C_{b'}$	148.323	148.277	148.277
C_c	156.875	156.882	156.882
$C_{c'}$	156.798	156.798	156.798
C_2	151.334	150.369	151.587
C_3	124.182	127.073	126.759
C_4	136.912	140.169	140.698
C_6	127.916	129.096	129.020
C_7	132.437	136.330	136.821
C_8	124.000	127.073	126.759
C_9	150.698	150.124	151.265
C_{H1}	43.998	43.983	43.983
C_{H2}	37.653	37.638	37.638
C_{H3}, C_{H5}, C_{H6}, C_{H7}	22.825	22.818	22.818
	23.937	23.929	23.929
	28.573	28.565	28.565
	30.588	30.580	30.580
C_{H4}, C_{H8}	10.871	10.863	10.863
	14.358	14.350	14.350

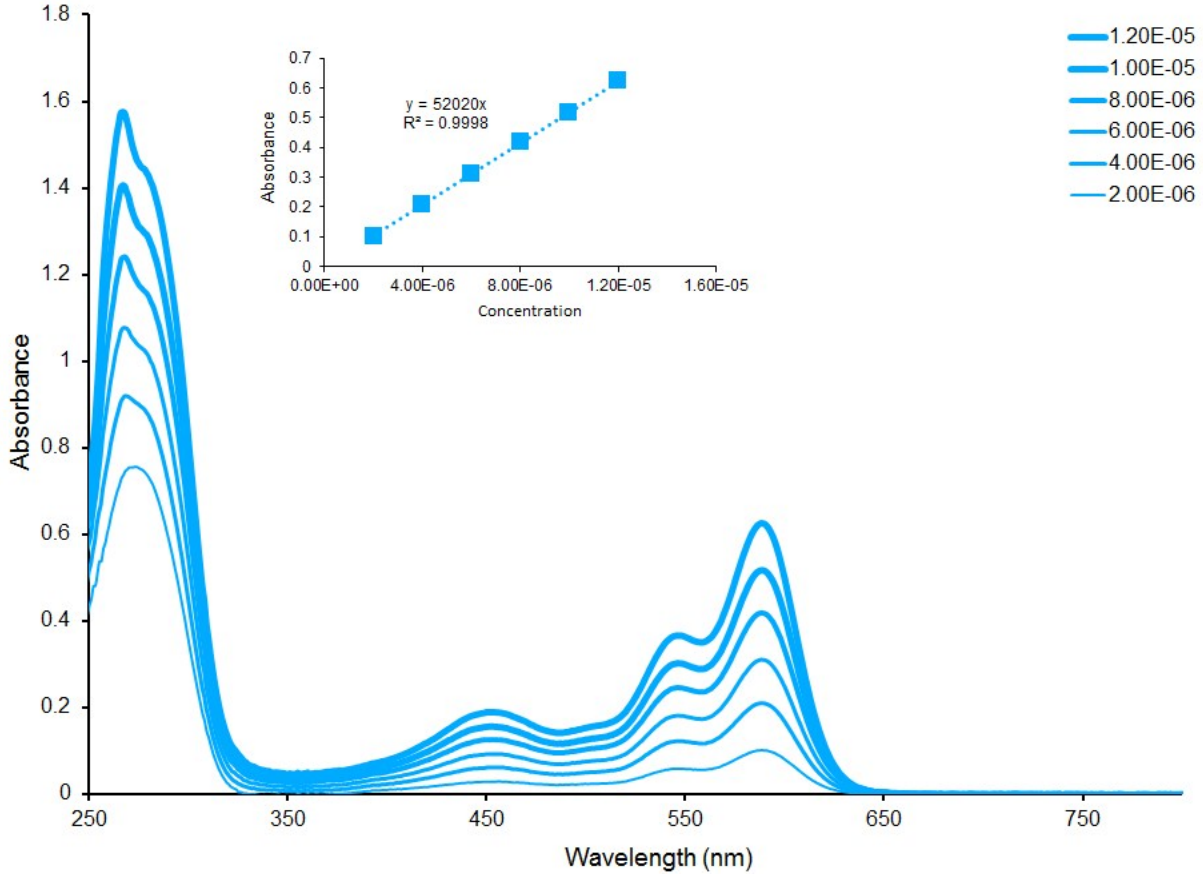

Figure S26. Electronic absorption spectra of **1** in DMSO at different concentrations (inset: plot of absorbance vs. concentration)

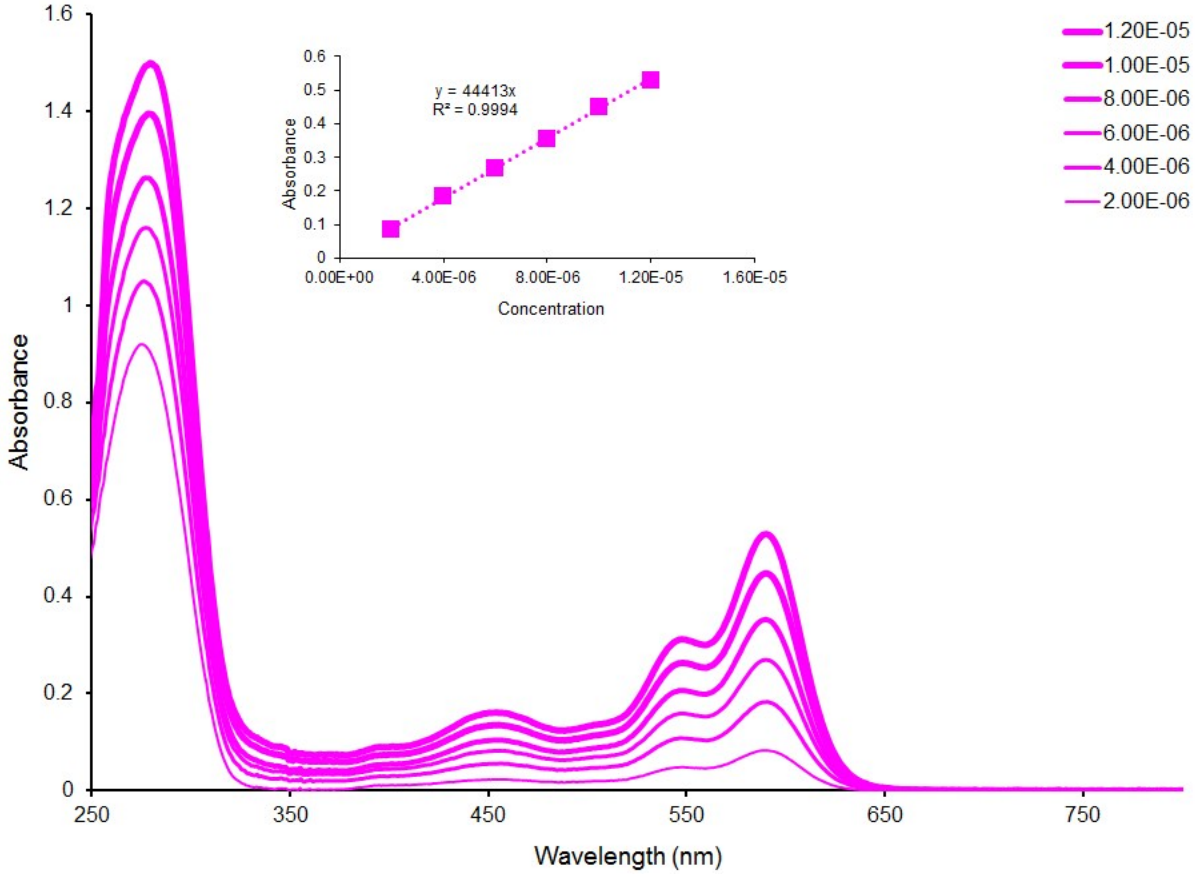

Figure S27. Electronic absorption spectra of **2** in DMSO at different concentrations (inset: plot of absorbance vs. concentration)

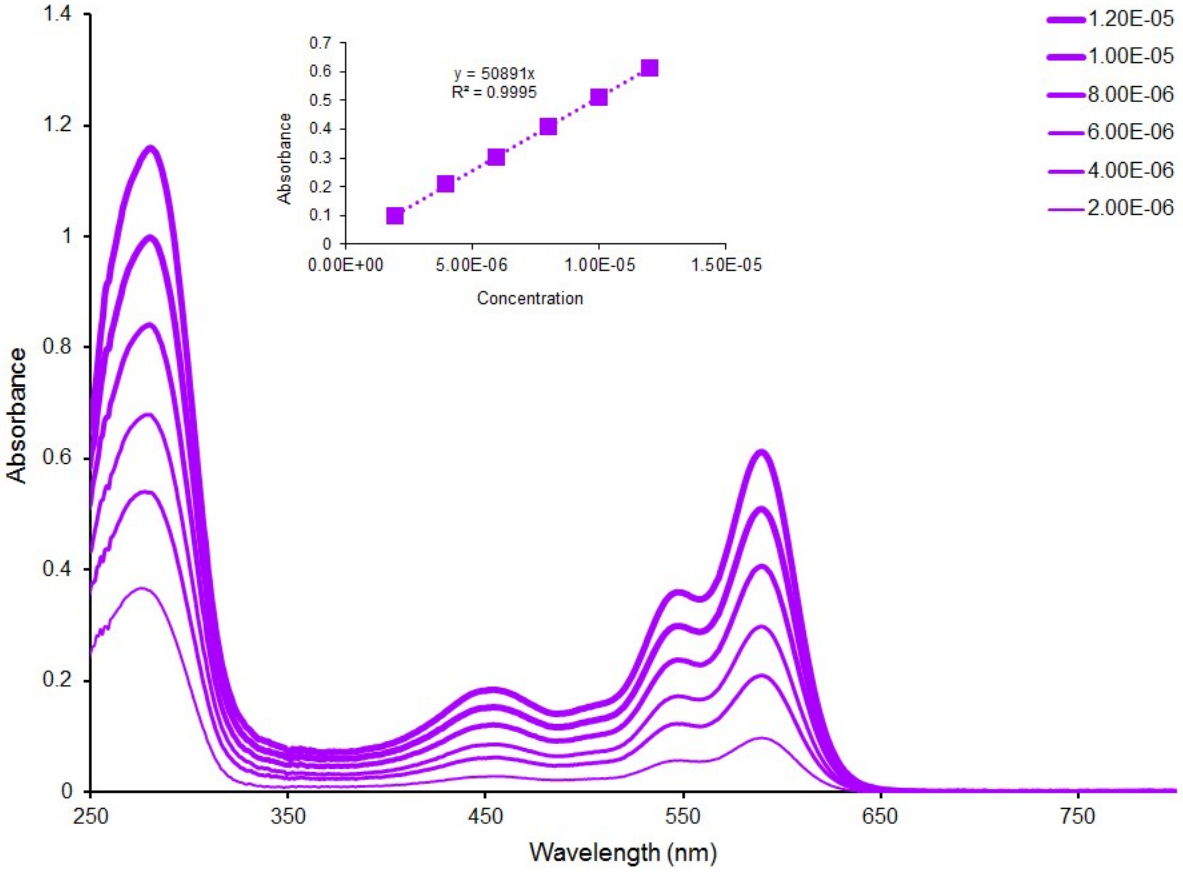

Figure S28. Electronic absorption spectra of **3** in DMSO at different concentrations (inset: plot of absorbance vs. concentration)

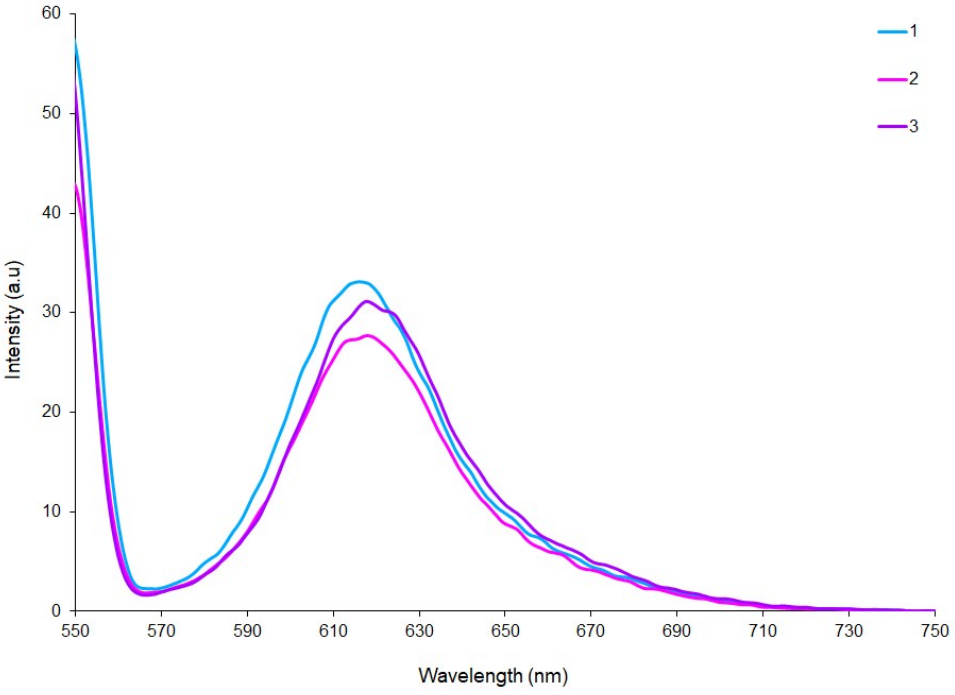

Figure S29. The fluorescence emission spectra of **1**, **2** and **3** in DMSO (1.0×10^{-5} M). (Excitation wavelength = 550 nm)

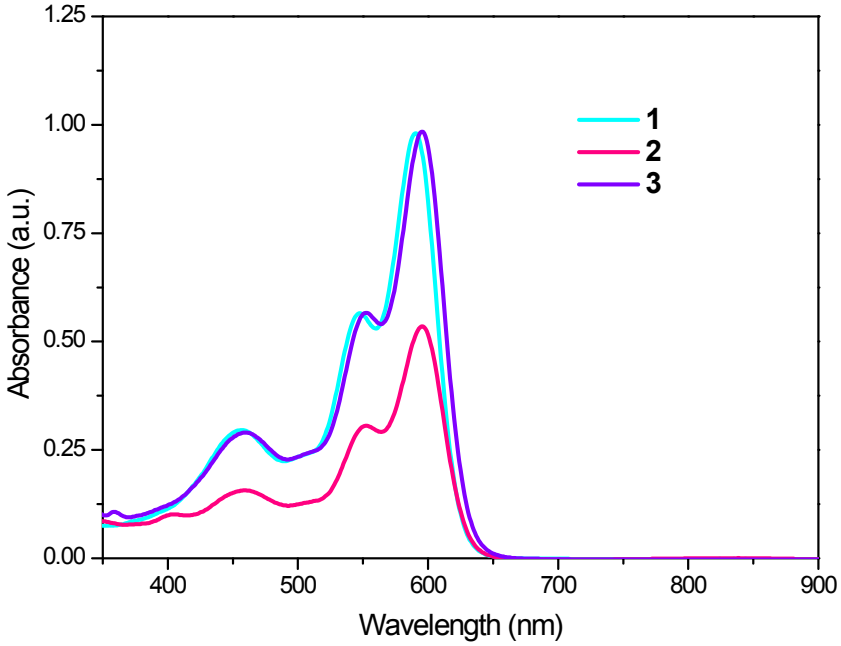

Figure S30. UV-Vis absorption spectra of **1**, **2** and **3** at $5x10^{-5}$ M in DCM.

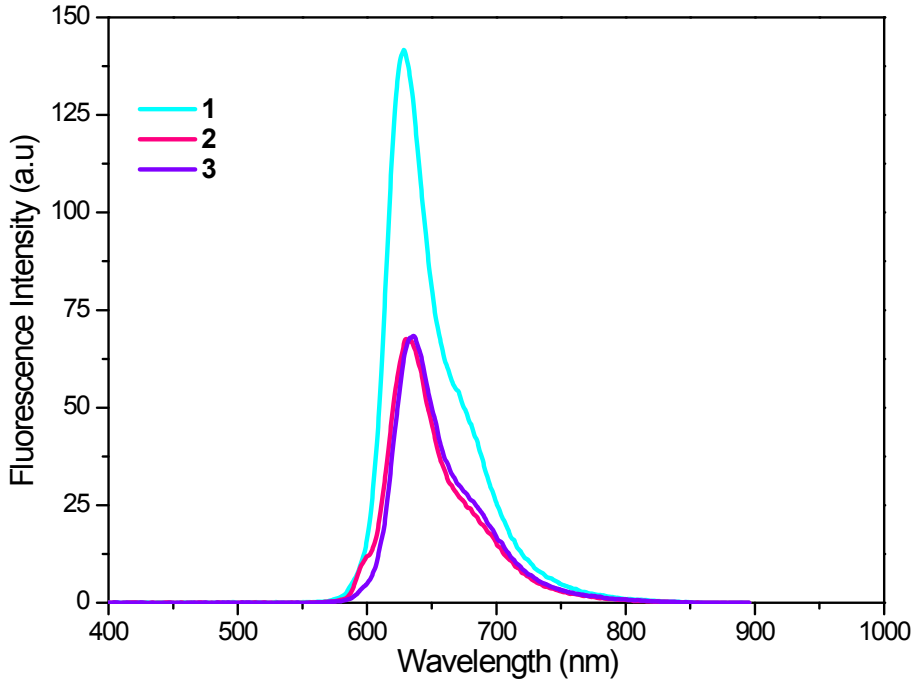

Figure S31. Fluorescence spectra of **1**, **2** and **3** at $5x10^{-5}$ M in DCM.

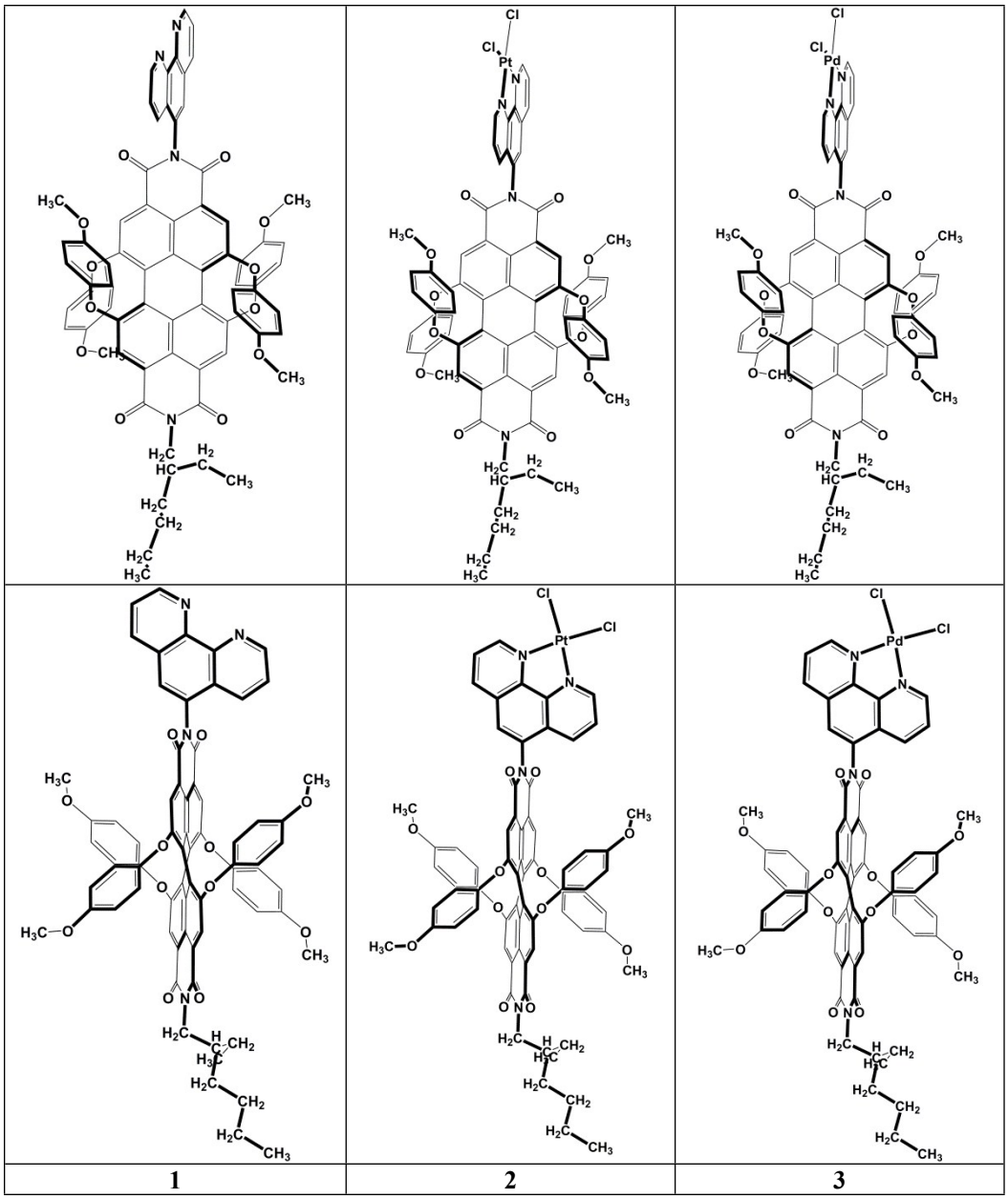

Figure S32. Schematic representation of the investigated molecules

Table S3. Dipole moments (μ, Debye), sum of electronic energies and zero-point energies (E_{elec}+ZPE, Hartree), complexation energies (ΔE_C) and some dihedral angles of studied systems calculated with B3LYP functional using 6-31G(d,p) and LANL2DZ (for metals) basis sets in DCM.

	μ (D)	E_{elec}+ZPE (Hartree)	[a]ΔE_C (kcal/mol)	Dihedral angle (C1C2C3C4)°	Dihedral angle (C5N1C6C7)°
1	5.36	-3898.118026		-28	90
2	21.07	-4937.737230	-25.92	-28	89
3	21.15	-4945.310683	-15.25	-28	92
$PtCl_2$	6.06	-1039.577881			
$PdCl_2$	6.28	-1047.168343			

[a]$\Delta E_C = [(E+ZPE)_{\mathbf{2/3}} - (E+ZPE)_{\mathbf{1}} - (E+ZPE)_{MCl2}]$

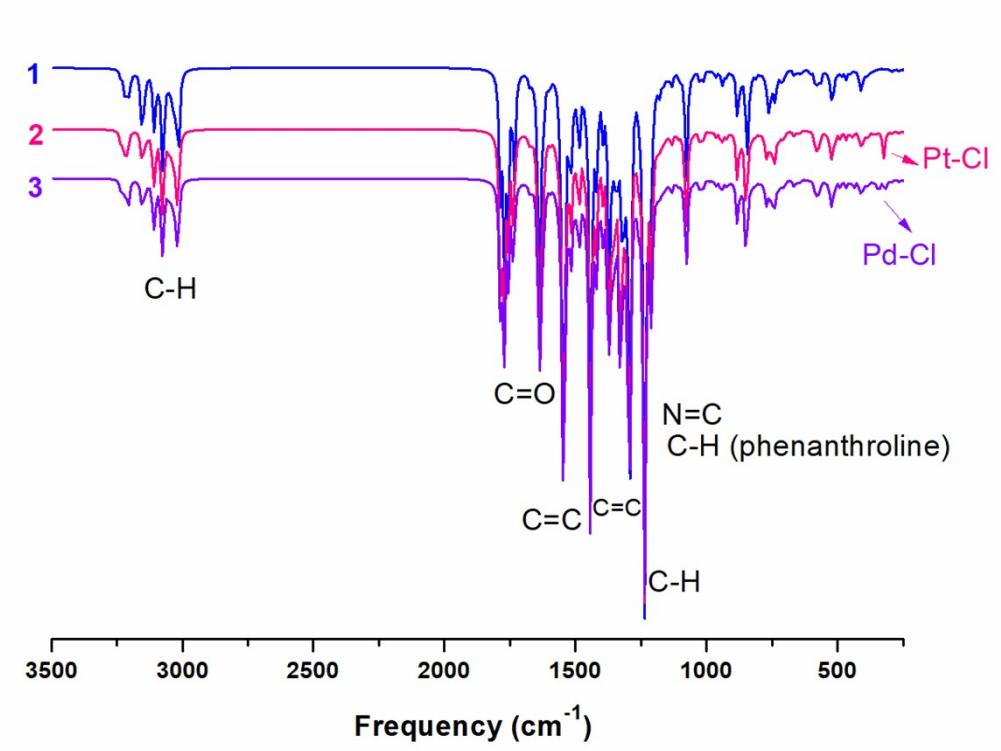

Figure S33. Calculated IR spectra of **1, 2** and **3** in gas phase.

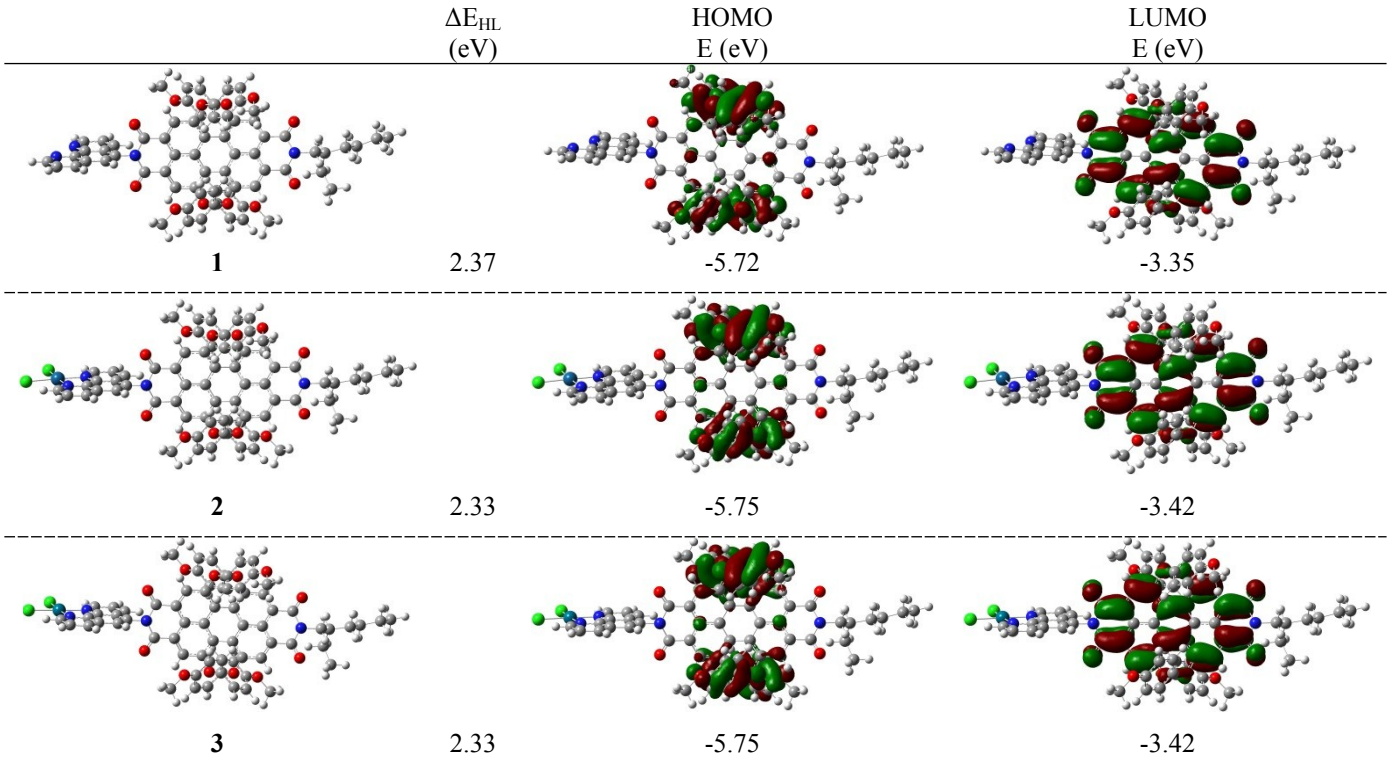

Figure S34. Frontier molecular orbitals, their energies, and HOMO-LUMO energy gaps for the investigated molecules calculated at B3LYP functional using 6-31G(d,p) and LANL2DZ (for metals) basis sets in DCM.

Table S4. Electronic transitions (λ_{ex}), oscillator strengths (f), transition dipole moments (μ_{tr}), excitation character, molecular orbitals and their % contributions of **1** at B3LYP/6-31G(d,p) level in DCM.

state	λ_{ex} (nm)	f	μ_{tr} (D)	Character[a]	Predominant Transitions	%
S_1	661	0.0416	0.9048	ICT1	H→L	70
S_2	640	0.0019	0.0393	ICT1	H-2→L	68
S_3	629	0.0632	1.3087	LE1,ICT1	H-1→L	62
				LE1,ICT1	H-4→L	27
S_4	620	0.0233	0.4750	ICT1	H-3→L	70
S_5	543	0.5563	9.5352	LE1,ICT1	H-4→L	65
S_6	447	0.0002	0.0025	ICT2	H-5→L	70
S_7	400	0.0321	0.4227	LE1,ICT3	H-8→L	62
S_8	398	0.0102	0.1332	ICT1	H→L+1	64
S_9	394.2	0.0062	0.0803	ICT2	H-6→L	46
				LE1,ICT1	H-1→L+1	40
S_{10}	394	0.0355	0.4610	LE1,ICT1	H-9→L	47
				ICT2	H-6→L	46
S_{11}	393	0.0279	0.3608	LE1,ICT1	H-1→L+1	45
				LE1,ICT3	H-9→L	37
S_{12}	388	0.0089	0.1138	ICT1	H-2→L+1	69
S_{13}	386	0.0032	0.0401	ICT1	H-10→L	61
				LE+ICT1	H-1→L+1	29
S_{14}	382.4	0.0077	0.0975	ICT1	H-11→L	65
S_{15}	382	0.0010	0.0132	ICT2	H-7→L	66
S_{16}	381	0.0004	0.0054	ICT1	H-3→L+1	65
S_{17}	380	0.0025	0.0314	ICT1	H-12→L	70
S_{18}	376	0.0158	0.1961	ICT1	H-13→L	69
S_{19}	369	0.0004	0.0049	LE1,ICT4	H-15→L	51
				LE1,ICT4	H-16→L	43
S_{20}	366	0.0001	0.0009	LE1,ICT1	H-4→L+1	66

[a]LE1: local excitation of perylene; ICT1: intramolecular charge-transfer from phenyl rings to perylene moiety; ICT2: intramolecular charge-transfer from phenanthroline to perylene moiety; ICT3: intramolecular charge-transfer from perylene to phenyl rings; ICT4: intramolecular charge-transfer from C=O, N and alkyl chain of perylene side to perylene.

Table S5. Electronic transitions (λ_{ex}), oscillator strengths (f), transition dipole moments (μ_{tr}), excitation character, molecular orbitals and their % contributions of **2** calculated at B3LYP functional using 6-31G(d,p) and LANL2DZ (for metals) basis sets in DCM.

state	λ_{ex} (nm)	f	μ_{tr} (D)	Character[a]	Predominant Transitions	%
S_1	679	0.0581	1.2975	ICT1	H→L	70
S_2	653	0.0119	0.2549	ICT1	H-2→L	60
				LE1,ICT1	H-1→L	37
S_3	646	0.1038	2.2068	LE1,ICT1	H-1→L	57
				ICT1	H-2→L	37
S_4	634	0.0335	0.6981	ICT1	H-3→L	70
S_5	563	0.6902	12.7975	LE1,ICT1	H-4→L	68
S_6	453	0.0001	0.0014	LMCT1,ICT5	H→L+1	62
S_7	448	0.0002	0.0023	LMCT2,ICT5	H-1→L+1	61
S_8	439	0.0000	0.0006	LMCT1,ICT5	H-2→L+1	66
S_9	436	0.0000	0.0003	MLCT1	H-5→L	71
S_{10}	431	0.0001	0.0011	LMCT1,ICT5	H-3→L+1	69
S_{11}	425	0.0001	0.0013	LMCT1,ICT5	H→L+2	65
S_{12}	423.3	0.0002	0.0027	LMCT2,ICT5	H-1→L+2	62
S_{13}	423	0.0001	0.0011	MLCT1,ICT2	H-6→L	70
S_{14}	418	0.0034	0.0463	LE2,MLCT3	H-5→L+1	66
S_{15}	414	0.0006	0.0084	LMCT2,ICT5	H-4→L+1	65
S_{16}	413	0.0000	0.0004	ICT5	H-2→L+2	63
S_{17}	407	0.0673	0.9020	LE1,ICT1	H-9→L	67
S_{18}	406	0.0004	0.0047	ICT5	H-3→L+2	69
S_{19}	405	0.0001	0.0010	MLCT2	H-7→L	70
S_{20}	404	0.0036	0.0479	LE2,MLCT3	H-7→L+1	65
S_{40}	363	0.1946	2.3306	LE2,MLCT3	H-5→L+1	56

[a]LE1: local excitation of perylene; LE2: local excitation of Pt; LMCT1: charge transfer from phenyl units to Pt; LMCT2: charge transfer from perylene to Pt; MLCT1: charge transfer from Pt-Cl2 to perylene; MLCT2: charge transfer from Pt to perylene; MLCT3: charge transfer from Pt-Cl2 to phenanthroline; ICT1: intramolecular charge-transfer from phenyl rings to perylene moiety; ICT5: intramolecular charge-transfer from phenyl rings to phenanthroline.

Table S6. Electronic transitions (λ_{ex}), oscillator strengths (f), transition dipole moments (μ_{tr}), excitation character, molecular orbitals and their % contributions of **3** calculated at B3LYP functional using 6-31G(d,p) and LANL2DZ (for metals) basis sets in DCM.

state	λ_{ex} (nm)	f	μ_{tr} (D)	Character[a]	Predominant Transitions	%
S_1	678.5	0.0590	1.3178	ICT1	H→L	71
S_2	653	0.0126	0.2712	ICT1	H-2→L	60
				LE1,ICT1	H-1→L	37
S_3	646	0.1036	2.2028	LE+ICT1	H-1→L	57
				ICT1	H-2→L	37
S_4	634	0.0334	0.6962	ICT1	H-3→L	70
S_5	563	0.6871	12.738	LE1,ICT1	H-4→L	68
S_6	486	0.0002	0.0025	LE2,MLCT3	H-5→L+1	66
S_7	485	0.0014	0.0001	LE2,MLCT3	H-8→L+1	62
S_8	461	0.0000	0.0001	LE2,MLCT3	H-6→L+1	66
S_9	458	0.0016	0.0243	LE2,MLCT3	H-13→L+1	64
S_{10}	452	0.0000	0.0001	LMCT1,ICT5	H→L+1	67
S_{11}	447	0.0000	0.0001	LMCT2,ICT5	H-1→L+1	66
S_{12}	446	0.0001	0.0014	ICT5	H→L+2	62
S_{13}	442	0.0001	0.0018	LMCT2,ICT5	H-1→L+2	61
S_{14}	440	0.0000	0.0002	LMCT1,ICT5	H-2→L+1	68
S_{15}	433	0.0000	0.0007	ICT5	H-2→L+2	66
S_{16}	432	0.0000	0.0002	LMCT1,ICT5	H-3→L+1	69
S_{17}	425	0.0001	0.0011	ICT5	H-3→L+2	69
S_{18}	419	0.0001	0.0018	ICT5	H→L+2	65
S_{19}	418	0.0002	0.0030	LMCT2,ICT5	H-1→L+2	62
S_{20}	413	0.0000	0.0002	LMCT2,ICT5	H-4→L+1	70

[a]LE1: local excitation of perylene; LE2: local excitation of Pd; LMCT1: charge transfer from phenyl units to Pd; LMCT2: charge transfer from perylene to Pd; MLCT1: charge transfer from Pd-Cl2 to perylene; MLCT2: charge transfer from Pd to perylene; MLCT3: charge transfer from Pd-Cl2 to phenanthroline; ICT1: intramolecular charge-transfer from phenyl rings to perylene moiety; ICT5: intramolecular charge-transfer from phenyl rings to phenanthroline.

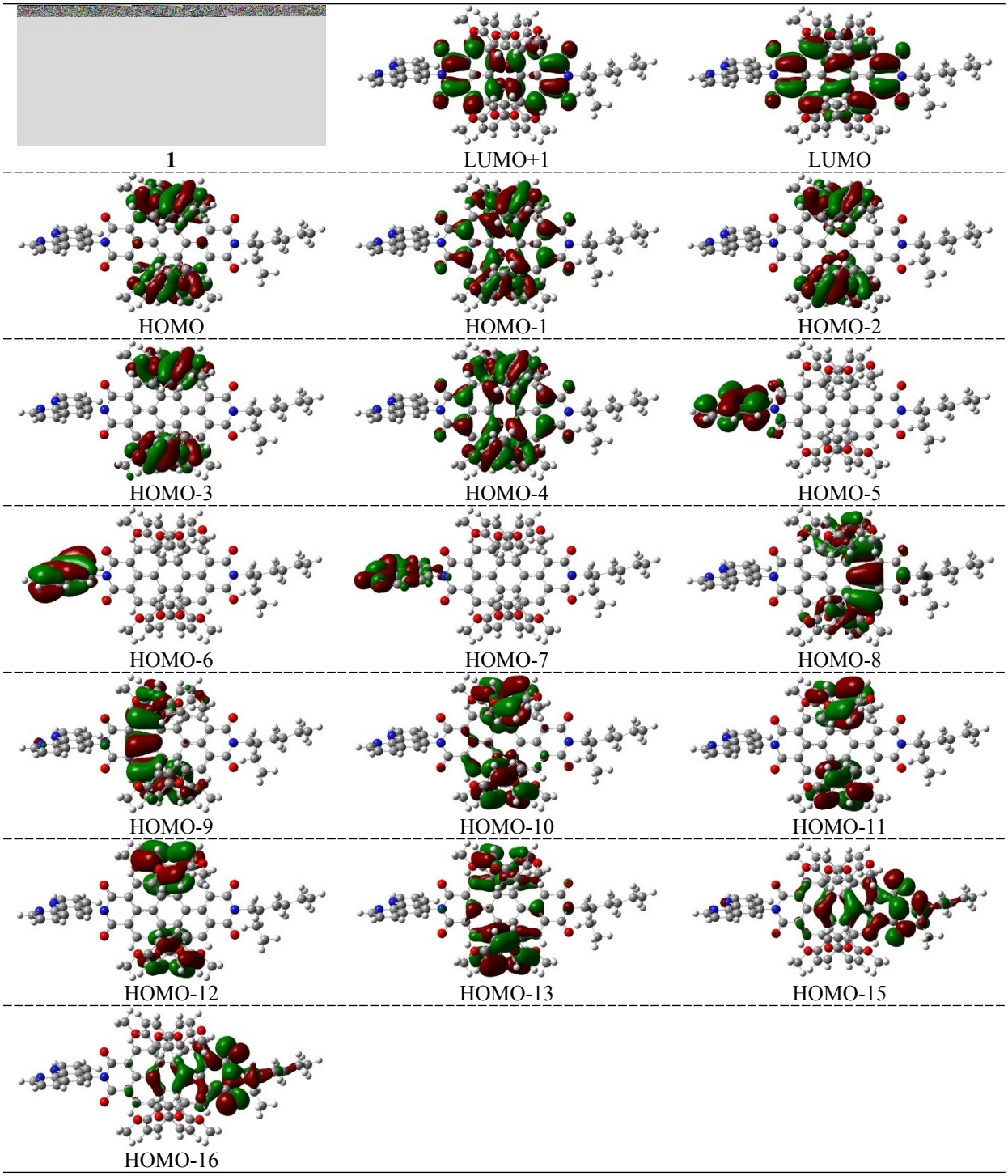

Figure S34. Selected molecular orbitals of **1** in DCM

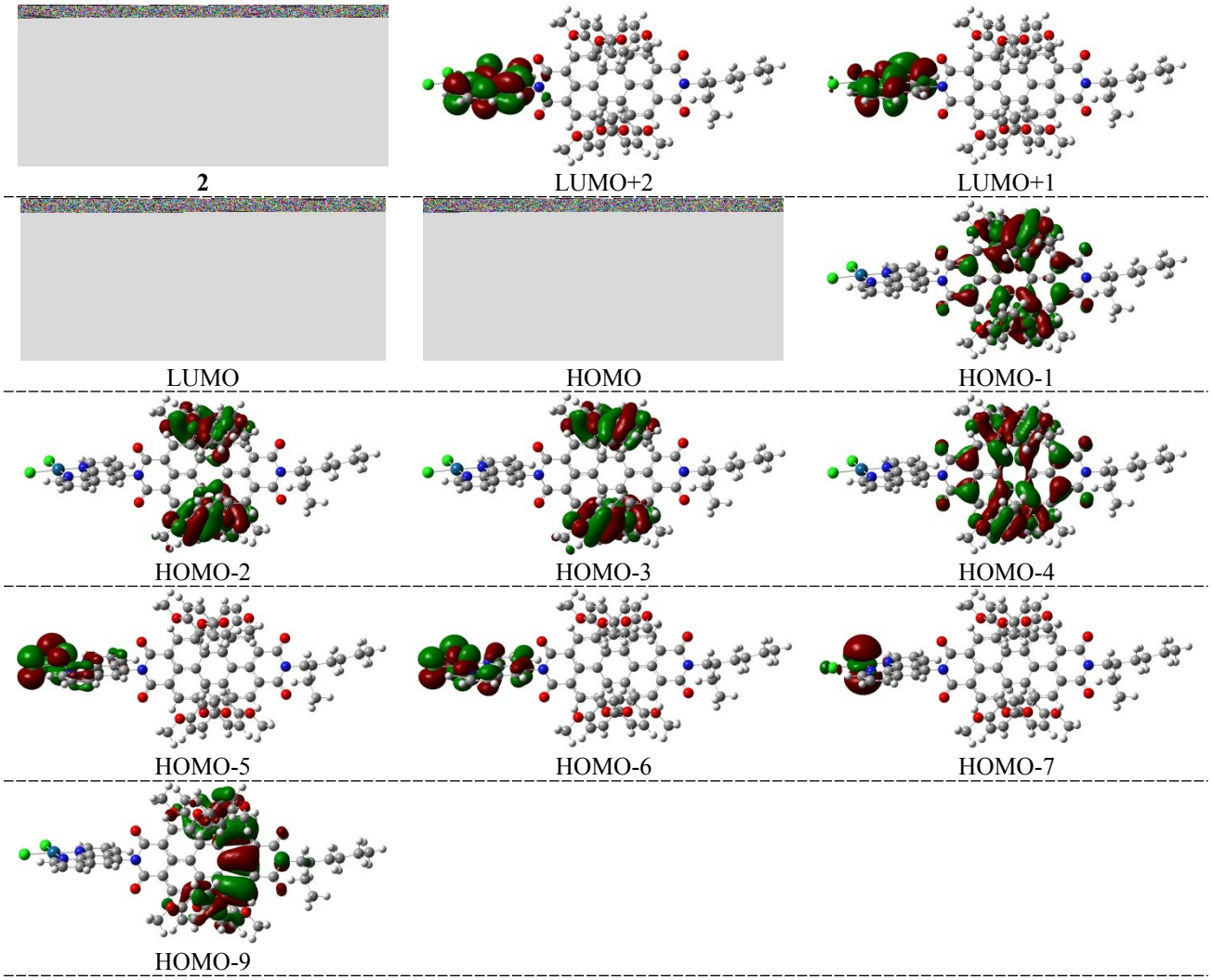

Figure S35. Some molecular orbitals of **2** in DCM.

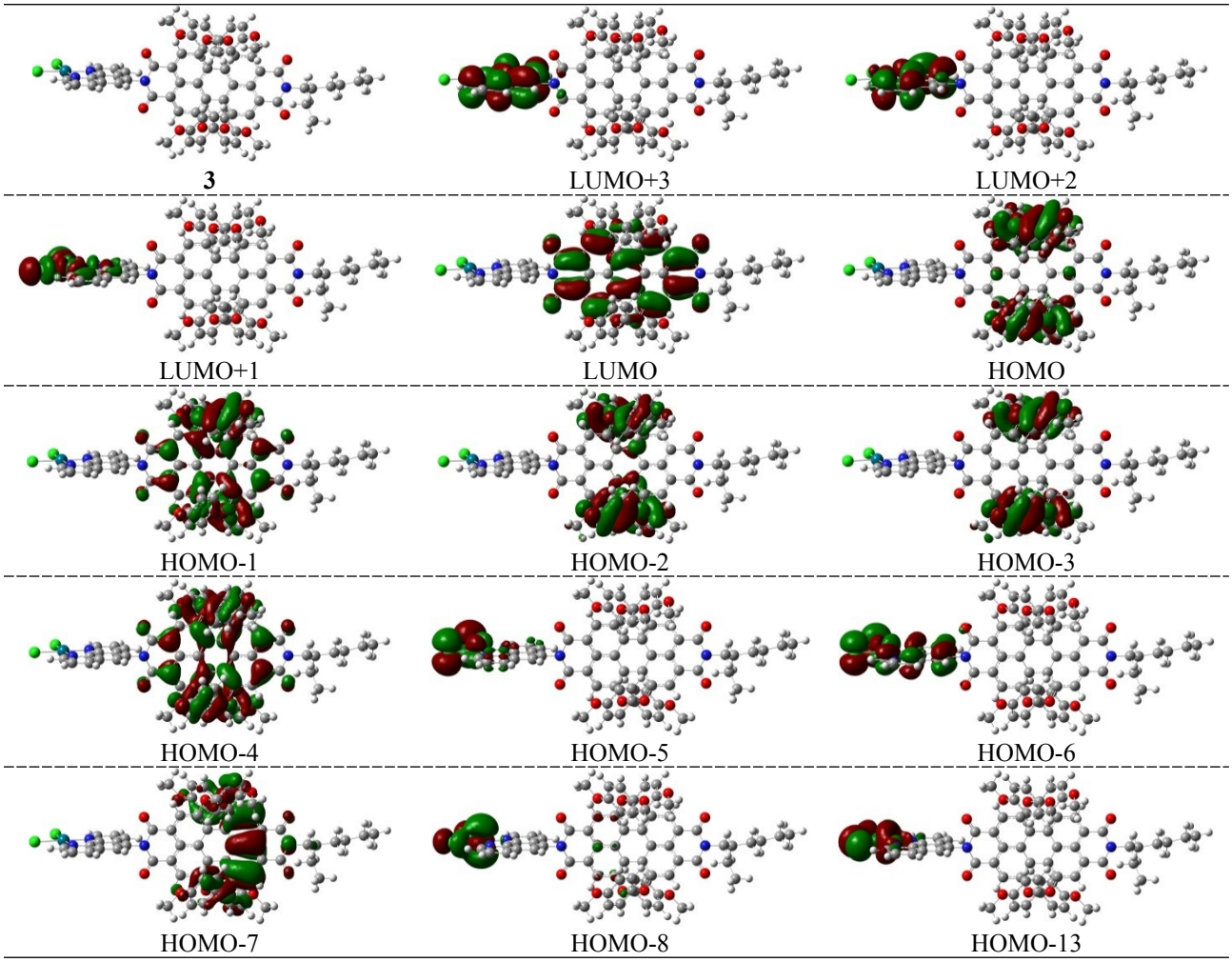

S36. Selected molecular orbitals of **3** in DCM.

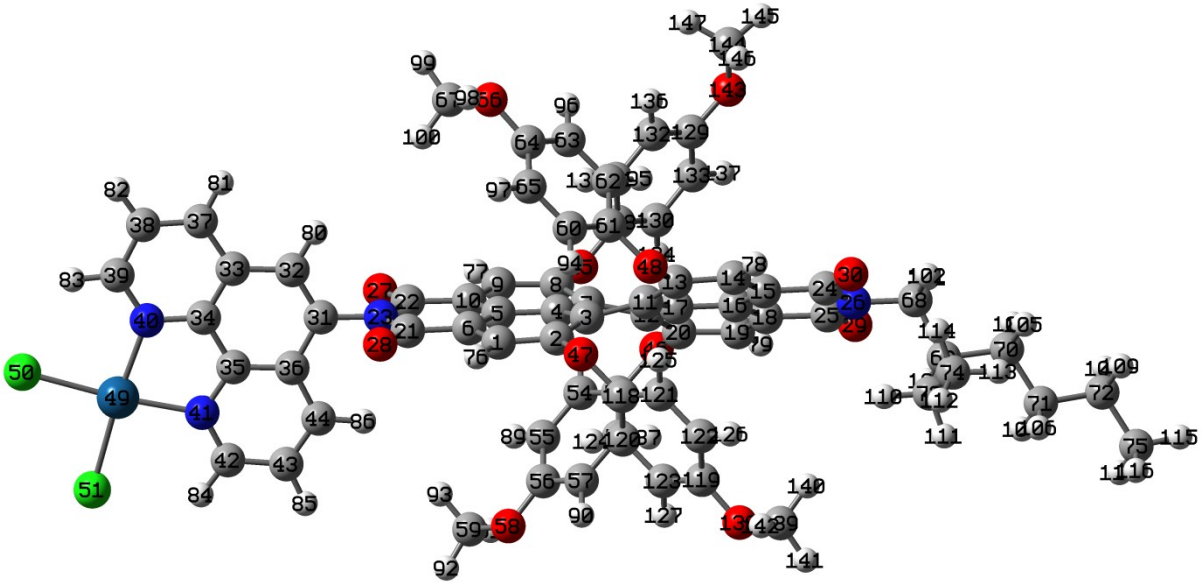

Table S7. Charge distribution in compound **2** in DCM

	Mulliken charges	NBO charges
Pt (49)	0.264	0.378
Cl (50)	-0.333	-0.477
Cl (51)	-0.334	-0.478
N (40)	-0.647	-0.415
N (41)	-0.643	-0.415
C (42)	0.130	0.087
C (43)	-0.111	-0.252
O (28)	-0.484	-0.639
C (31)	0.203	0.199
N (23)	-0.621	-0.508
C (21)	0.487	0.695
C (22)	0.487	0.694
O (27)	-0.485	-0.640
O (28)	-0.484	-0.639
O (58)	-0.486	-0.502

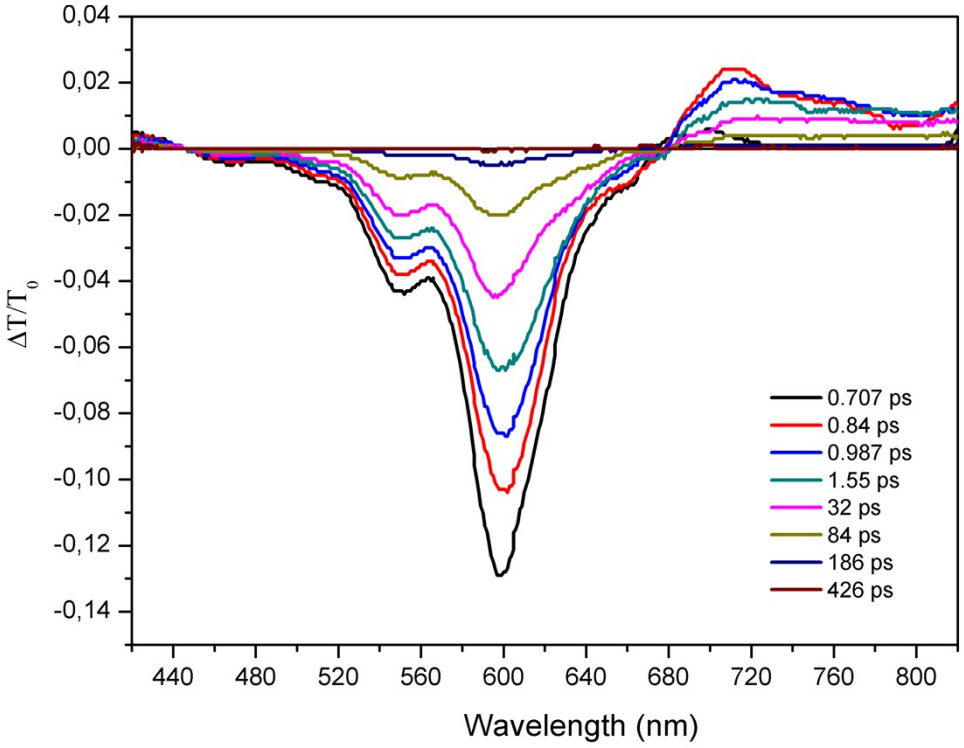

Figure S37. Ultrafast transient absorption spectra of **2** with different time delays at excited 590 nm femtosecond pulsed laser

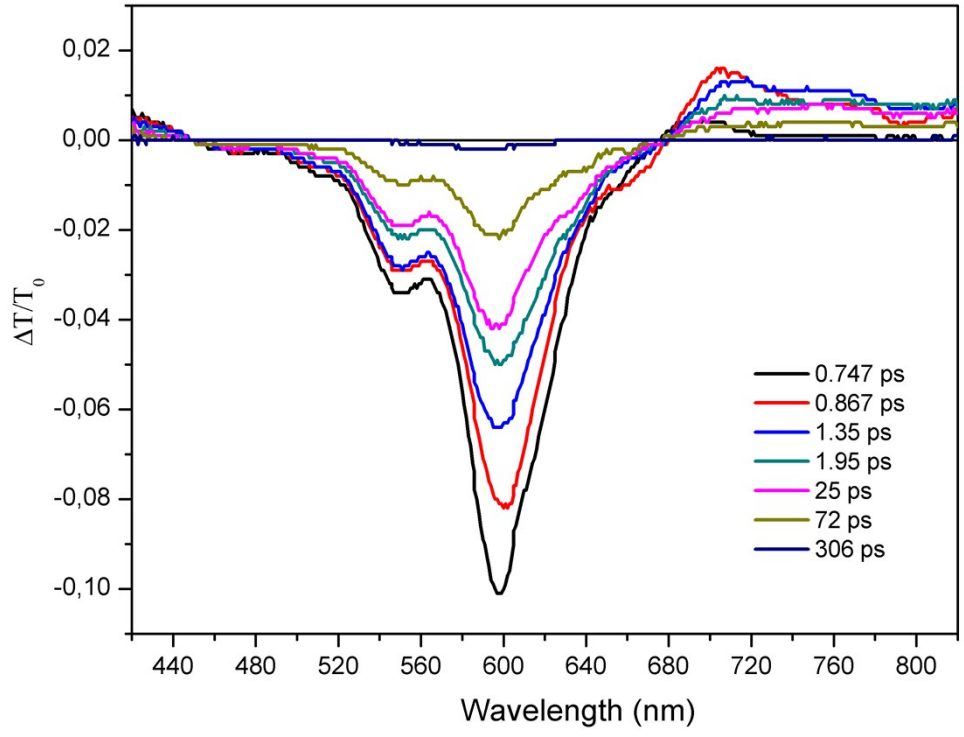

Figure S38. Ultrafast transient absorption spectra of **3** with different time delays at excited 590 nm femtosecond pulsed laser